Accepted Manuscript

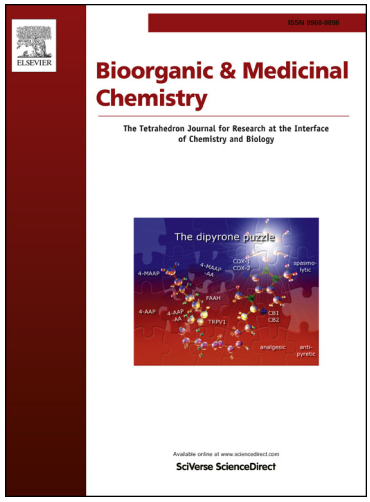

Synthesis, molecular docking and biological evaluation of *N*,*N*-disubstituted 2–aminothiazolines as a new class of butyrylcholinesterase and carboxylesterase inhibitors

Galina F. Makhaeva, Natalia P. Boltneva, Sofya V. Lushchekina, Olga G. Serebryakova, Tatyana S. Stupina, Alexey A. Terentiev, Igor V. Serkov, Alexey N. Proshin, Sergey O. Bachurin, Rudy J. Richardson

PII: S0968-0896(16)30033-5
DOI: http://dx.doi.org/10.1016/j.bmc.2016.01.031
Reference: BMC 12774

To appear in: *Bioorganic & Medicinal Chemistry*

Received Date: 5 November 2015
Revised Date: 4 January 2016
Accepted Date: 17 January 2016

Please cite this article as: Makhaeva, G.F., Boltneva, N.P., Lushchekina, S.V., Serebryakova, O.G., Stupina, T.S., Terentiev, A.A., Serkov, I.V., Proshin, A.N., Bachurin, S.O., Richardson, R.J., Synthesis, molecular docking and biological evaluation of *N*,*N*-disubstituted 2–aminothiazolines as a new class of butyrylcholinesterase and carboxylesterase inhibitors, *Bioorganic & Medicinal Chemistry* (2016), doi: http://dx.doi.org/10.1016/j.bmc.2016.01.031

Synthesis, molecular docking and biological evaluation of *N,N*-disubstituted 2-aminothiazolines as a new class of butyrylcholinesterase and carboxylesterase inhibitors

Galina F. Makhaeva[a], Natalia P. Boltneva[a], Sofya V. Lushchekina[a,b], Olga G. Serebryakova[a], Tatyana S. Stupina[c], Alexey A. Terentiev[c], Igor V. Serkov[a], Alexey N. Proshin[a], Sergey O. Bachurin[a], Rudy J. Richardson[d]*

[a] *Institute of Physiologically Active Compounds Russian Academy of Sciences, Chernogolovka, 142432, Russia*

[b] *Emanuel Institute of Biochemical Physics Russian Academy of Sciences, Moscow, 119334, Russia*

[c] *Institute of Problems of Chemical Physics Russian Academy of Sciences, Chernogolovka, 142432, Russia*

[d] *Department of Environmental Health Sciences and Department of Neurology, University of Michigan, Ann Arbor, MI 48109 USA*

* Corresponding author:

Dr. Rudy J. Richardson
Computational Toxicology Laboratory
Toxicology Program
Department of Environmental Health Sciences
University of Michigan
Ann Arbor, Michigan 48109-2029 USA

E-mail: rjrich@umich.edu
Tel: +1-734-936-0769
Fax: +1-734-763-8095

Abstract

A series of 31 *N*,*N*-disubstituted 2-amino-5-halomethyl-2-thiazolines was designed, synthesized, and evaluated for inhibitory potential against acetylcholinesterase (AChE), butyrylcholinesterase (BChE) and carboxylesterase (CaE). The compounds did not inhibit AChE; the most active compounds inhibited BChE and CaE with IC_{50} values of 0.22 to 2.3 μM. Pyridine-containing compounds were more selective toward BChE; compounds with the para-OMe substituent in one of the two dibenzyl fragments were more selective toward CaE. Iodinated derivatives were more effective BChE inhibitors than brominated ones, while there was no influence of halogen type on CaE inhibition. Inhibition kinetics for the 9 most active compounds indicated non-competitive inhibition of CaE and varied mechanisms (competitive, non-competitive, or mixed-type) for inhibition of BChE. Docking simulations predicted key binding interactions of compounds with BChE and CaE and revealed that the best docked positions in BChE were at the bottom of the gorge in close proximity to the catalytic residues in the active site. In contrast, the best binding positions for CaE were clustered rather far from the active site at the top of the gorge. Thus, the docking results provided insight into differences in kinetic mechanisms and inhibitor activities of the tested compounds. A cytotoxicity test using the MTT assay showed that within solubility limits (< 30 μM), none of the tested compounds significantly affected viability of human fetal mesenchymal stem cells. The results indicate that a new series of *N*,*N*-disubstituted 2-aminothiazolines could serve as BChE and CaE inhibitors for potential medicinal applications.

Keywords

N,*N*-disubstituted 2-aminothiazolines, acetylcholinesterase, butyrylcholinesterase, carboxylesterase, molecular docking, Alzheimer's Disease.

1. Introduction

Among functional types of enzymes, serine hydrolases constitute one of the largest and most varied groups. Of the approximately 240 serine hydrolases found in humans, about half are serine proteases whereas the remainder carry out metabolic functions. The metabolic serine hydrolases include diverse lipases, peptidases, esterases, thioesterases, and amidases that hydrolyze small molecules, peptides, or post-translational (thio)ester protein modifications [1]. Because these enzymes serve important physiological and pathogenic functions and their mechanisms of action are well understood, they have been popular targets for drug development [2, 3].

Acetylcholinesterase (AChE, EC 3.1.1.7) is a metabolic serine hydrolase that catalyzes the hydrolysis of acetylcholine, thus regulating cholinergic neurotransmission. Therefore, in disorders such as Alzheimer's disease (AD), where there is diminished cholinergic activity, inhibition of AChE has been employed to treat some of the symptoms attributed to decreased acetylcholine levels [4, 5]. Most of the currently available drugs on the market (tacrine, donepezil, rivastigmine and galanthamine) intended to treat AD are AChE inhibitors [4-6].

However, during the progression of Alzheimer's disease, brain AChE levels decline while butyrylcholinesterase (BChE, EC 3.1.1.8) activity increases, suggesting that acetylcholine hydrolysis may occur to a greater extent via BChE catalysis [7, 8]. In this regard, it has been reported that highly selective inhibition of BChE is important in raising acetylcholine levels and improving cognition [8-12]. Because selective BChE inhibitors do not exhibit the adverse cholinergic effects of AChE inhibitors, the search for selective BChE inhibitors is currently a promising direction in medicinal chemistry research [10, 13-15]. Moreover, whereas some of the anticholinesterase compounds currently employed for AD treatment can inhibit both AChE and BChE [12, 16], the highly selective AChE inhibitor (-) huperzine A was clinically ineffective[17]. Likewise, the selective AChE inhibitor (-) phenserine was found to be potentially efficacious for mild to moderate AD, but because this drug also inhibits production of amyloid precursor protein, it is difficult to assess the degree to which its efficacy stems from AChE inhibition [18]. Taken together, these findings suggest that the development of selective BChE inhibitors could be important for more effective treatment of AD [19].

In recent years, interest in another group of metabolic hydrolases, the carboxylesterases (CaE, EC 3.1.1.1), has sharply increased. CaE play major roles in the activation, detoxification and biodistribution of xenobiotics and numerous classes of drugs including

esters, thioesters, carbamates, and amides [20, 21]. Representative types of pharmaceutical agents include angiotensin-converting enzyme inhibitors, angiotensin receptor blockers, antiplatelet drugs, statins, antivirals, and central nervous system agents [22]. Inhibitors of CaE decrease the rate of hydrolysis of such drugs and thus reduce the rate of conversion of pro-drug to active drug or, conversely, increase the half-life of the active drug. Consequently, CaE inhibitors have important therapeutic value [23] and discovery of new CaE inhibitors with high selectivity is of considerable interest [24].

Recently, N,S-containing heterocyclic compounds, especially derivatives of 2-amino-1,3-thiazole, have attracted increasing attention due to their chemical and biological properties. For example, it has become known that many compounds containing the thiazoline (4,5-dihydro-1,3-thiazole) fragment exhibit antibacterial, anticancer, antifungal, and other types of biological activities [25-27]. However, information about the inhibition of serine esterases by compounds containing the thiazoline fragment is practically absent in the literature. The ability to reversibly inhibit cholinesterases was shown for only some 2-substituted thiazolines and imidazo[2,1-b]thiazole derivatives [28, 29].

Our preliminary study [30] showed that *N*,*N*-disubstituted-2-aminothiazolines could inhibit BChE and CaE while exhibiting minimal inhibitory activity against AChE. A search of chemical reactivity of 5-Br-methyl substituted thiazolines for the past 40 years using Reaxys turned up very few reactions. The alkylation reactions for 5-Br-methyl thiazolines were not described in the literature. The same results were obtained with SciFinder. Thus, the ability of 2-amino-5-halomethylthiazoline derivatives to alkylate DNA is unlikely. Therefore, we extended our experimental search for inhibitors of serine esterases with potential biomedical application in the 2-aminothiazoline series.

Here, we report the synthesis of 31 derivatives of 2-aminothiazolines of general formula shown in **Fig. 1**. The syntheses are outlined in **Scheme 1** and the structures of the individual compounds are listed in **Table 1**. Our strategy for the design of the inhibitors is illustrated in **Fig. 2**. We have also performed a biological evaluation of these compounds as inhibitors of three metabolic serine esterases (AChE, BChE and CaE) along with an optimization of their structures to yield selective inhibitors of BChE and/or CaE. To gain further insight into the molecular determinants responsible for the observed ability to inhibit BChE and CaE, molecular docking of the 9 most active compounds was carried out. In addition, the effect of the compounds on cell viability was evaluated in human fetal mesenchymal stem cells.

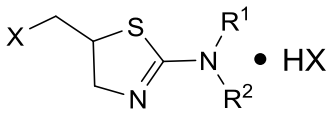

Figure 1. General structure of compounds in the present study. X = Br or I; R^1 = substituted or unsubstituted aryl or aralkyl; R^2 = H, aryl, or aralkyl. Note that the structure depicts the hydrohalide salt of the compounds. Syntheses are depicted in **Scheme 1** and structures of individual compounds are listed in **Table 1**.

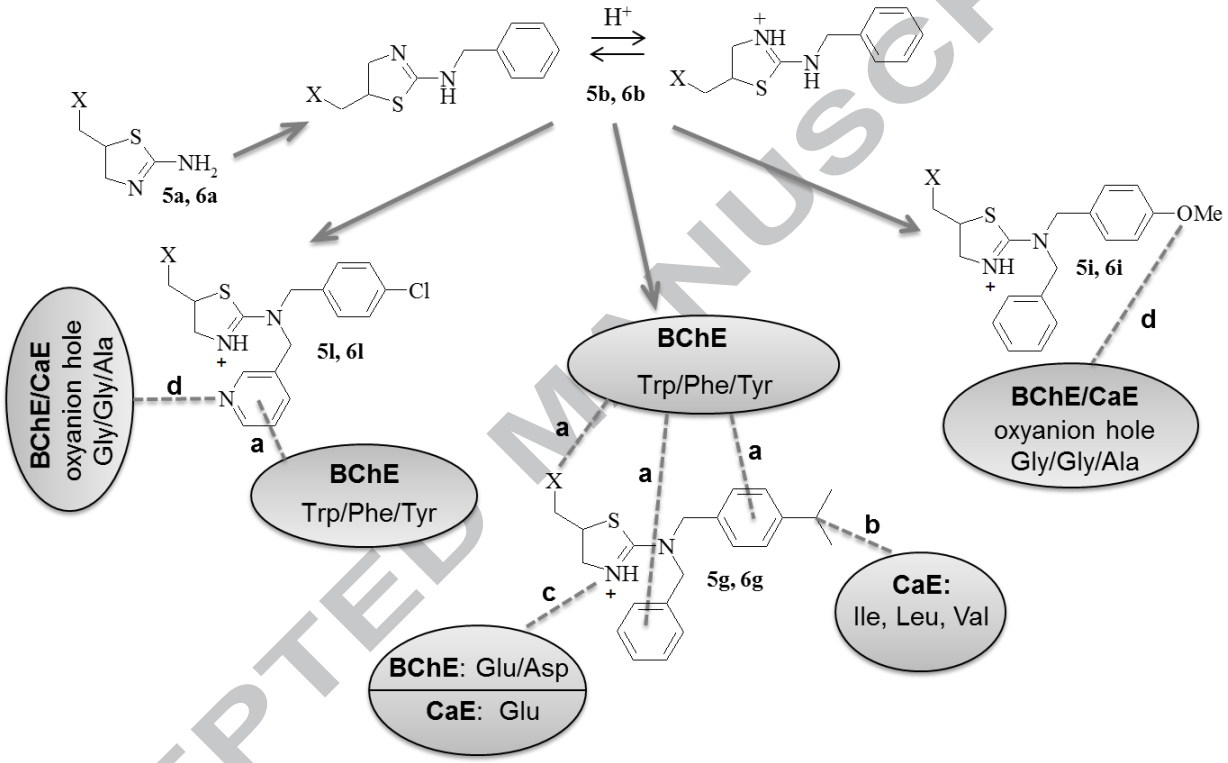

Figure 2. Design strategy for the new series of *N*,*N*-disubstituted 2-aminothiazolines of general formula shown in Fig. 1. X = Br or I. Syntheses are depicted in **Scheme 1** and structures of the compounds are presented in **Table 1**. Proposed interactions of compounds with active site residues of target enzymes include the following, illustrated with selected compounds: (**a**) Halogen and aromatic (benzyl, pyridine) fragments are intended to have stacking interactions with aromatic Trp, Phe and Tyr residues, primarily the most favorably oriented Trp82 and Trp231 of BChE; (**b**) Alkyl fragments are intended to interact with numerous hydrophobic residues lining the gorge of CaE; (**c**) Positively charged groups are intended to interact with Glu of both enzymes (Glu197 of BChE and Glu220 of CaE), and probably Asp70 of the peripheral anionic site of BChE; (**d**) Electronegative atoms (N, O) are expected to interact with the oxyanion hole of both enzymes (Gly116/Gly117/Ala199 for BChE and Gly142/Gly143/Ala222 for CaE).

2. Results and discussion

2.1. Chemistry.

We have synthesized the hydrohalides of 2-amino-substituted 5-halomethyl-2-thiazolines **5a-m** and **6a-t** by traditional methods (**Scheme 1**): iodination or bromination of the corresponding N',N'-derivatives of N-allylthiourea [31] obtained from allylisothiocyanate and the corresponding amine.

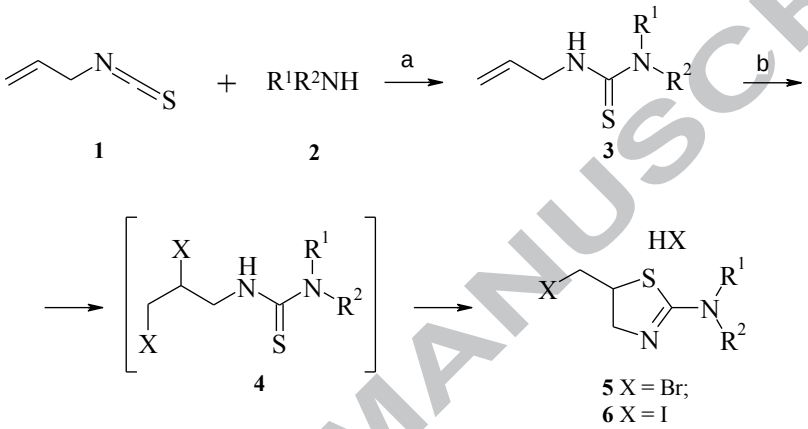

Scheme 1. Synthesis of *N,N*-disubstituted 2-aminothiazolines **5,6**. Reagents and conditions: (a) diethyl ether, r.t., 2–5 h, (b) X_2, CH_3OH, r.t., 24 h.

Previous studies have shown that isomeric six-membered rings (thiazines) are formed in these reactions as well as thiazolines [32, 33]. However, given that these reactions are usually performed in polar media with heating, only five-membered thiazoline ring compounds are isolated from the reaction mixture, because under these conditions there is a facile dihydrothiazine-thiazoline rearrangement [34]. The structural features of the synthesized compounds are shown in **Table 1**. Most of the compounds were synthesized for the first time for the present report, but we have previously reported [31] on the synthesis of 7 compounds: **6a, 6b, 6c, 6e, 6f, 6h, 6i, 6k**. All of the compounds except **5k, 6k** are racemic mixtures. Compounds **5k, 6k** are diastereomeric mixtures.

2.2. Inhibition studies of AChE, BChE and CaE (IC_{50}). Structure-activity relationships.

All 31 compounds were assessed for their potential to inhibit AChE, BChE and CaE by determining the IC_{50} – the inhibitor concentration that decreases the enzyme activity by half. AChE from human erythrocytes (RBCs) was used along with two enzymes of non-human

origin, namely BChE from equine serum and CaE from porcine liver because of their lower cost, high degree of identity with human enzymes, and the exploratory character of this work. Three drugs: tacrine, donepezil, and benzil (1,2-diphenylethane-1,2-dione) were used as positive controls [35]. The IC_{50} results are summarized in **Table 1**.

Table 1
Structures of the synthesized *N,N*-disubstituted 2-aminothiazolines and their inhibitory potencies (IC_{50}) toward AChE, BChE, and CaE.[a]

Cmpd	R^1	R^2	X	IC_{50} (μM)[b]		
				AChE (human RBC)	BChE (Equine serum)	CaE (Porcine Liver)
5a	H	H	Br	n.a.	n.a.	> 100
6a	H	H	I	n.a.	n.a.	n.a.
5b	H	Bn	Br	n.a.	29 ± 2	> 100
6b	H	Bn	I	n.a.	> 100	17 ± 1
5c	H	Ph	Br	n.a.	n.a.	> 100
6c	H	Ph	I	n.a.	n.a.	> 100
5d	H	pyridin-2-yl	Br	110 ± 10	63 ± 6	93 ± 5
6d	H	pyridin-2-yl	I	71 ± 7	2.74 ± 0.25	610 ± 60
5e	Bn	Bn	Br	n.a.	26 ± 1	32± 3
6e	Bn	Bn	I	n.a.	25 ± 1	46 ± 4
5f	Bn	4-$FC_6H_4CH_2$	Br	n.a.	38 ± 3	40 ± 4
6f	Bn	4-$FC_6H_4CH_2$	I	n.a.	17 ± 1	80 ± 8
5g	Bn	4-*i*-$PrC_6H_4CH_2$	Br	n.a.	11 ± 1	2.55 ± 0.23
6g	Bn	4-*i*-$PrC_6H_4CH_2$	I	n.a.	4.14 ± 0.39	2.13 ± 0.19
5h	Bn	4-*t*-$BuC_6H_4CH_2$	Br	n.a.	2.34 ± 0.21	0.32 ± 0.03
6h	Bn	4-*t*-$BuC_6H_4CH_2$	I	n.a.	0.77 ± 0.07	0.22 ± 0.02
5i	Bn	4-$MeOC_6H_4CH_2$	Br	n.a.	34 ± 3	4.90 ± 0.45
6i	Bn	4-$MeOC_6H_4CH_2$	I	n.a.	25 ± 1	4.66 ± 0.21
5k	Bn	CH(Me)Ph	Br	n.a.	14 ± 1	> 100
6k	Bn	CH(Me)Ph	I	n.a.	> 100	19 ± 2
5l	4-$ClC_6H_4CH_2$	pyridin-3-ylmethyl	Br	n.a.	30 ± 1	> 100
6l	4-$ClC_6H_4CH_2$	pyridin-3-ylmethyl	I	> 100	2.47 ± 0.22	18 ± 1
5	2-$ClC_6H_4CH_2$	pyridin-3-ylmethyl	Br	n.a.	25 ± 2	> 100
6	2-$ClC_6H_4CH_2$	pyridin-3-ylmethyl	I	n.a.	21 ± 1	> 100
6n	Bn	2-$ClC_6H_4CH_2$	I	n.a.	44 ± 3	117 ± 12
6o	Bn	3,4-$(MeO)_2C_6H_3CH_2$	I	> 100	20 ± 2	> 100
6p	Bn	3,5-(*t*-$Bu)_2$-4-OH-$C_6H_2CH_2$	I	n.a.	> 100	n.a.
6q	Bn	furan-2-yl	I	n.a.	42 ± 4	131 ± 12
6r	H	3,4-$OCH_2CH_2O)C_6H_3$	I	n.a.	> 100	> 100
6s	H	6-Me-pyridin-2-yl	I	n.a.	n.a.	n.a.
6t	H	dibenzofuran-3-yl	I	n.a.	> 100	> 100

Tacrine[c]			0.079 ± 0.002	0.034 ± 0.001 (human BChE)	> 100 (human CE1)
Donepezil[c]			0.022 ± 0.005	7.6 ± 1.3 (human BChE)	> 100 (human CE1)
Benzil[c,d]			> 100	> 100 (human BChE)	0.37 ± 0.04 (human CE1)

n.a. – not active
[a] General structure of the synthesized compounds is shown in **Fig. 1**.
[b] Data are means + SEM from 3 experiments.
[c] [35]; human CE1 = human liver carboxylesterase 1.
[d] 1,2-diphenylethane-1,2-dione

Comparing inhibitory potencies of a compound against the three esterase targets yields an esterase profile, which helps predict the main potential pharmacological effect of the compound and evaluate its possible side-effects, [36-39] thus helping to define the area(s) of potential application of the compound. For example, effective inhibitors of AChE and BChE can be used for AD treatment. However, inhibition of CaE by such anticholinesterase compounds leads to adverse drug-drug interactions [35]. On the other hand, potent and selective inhibitors of CaE can be used for the regulation of the metabolism and pharmacokinetics of ester-containing drugs [23, 24]. For such CaE inhibitors, anticholinesterase activity can be an undesirable side effect.

As seen from Table 1, most of the synthesized compounds did not substantially inhibit AChE, while the degree of BChE and CaE inhibition depended on structural features.

As starting templates for modification, we selected 5-bromomethyl-4,5-dihydro-thiazol-2-yl-amine (**5a**) and 5-iodomethyl-4,5-dihydro-thiazol-2-yl-amine (**6a**) that were not substituted on the outside nitrogen atom. These compounds were not active inhibitors: they did not inhibit AChE, BChE and weakly inhibited CaE (**5a**) (**Fig. 1**, **Table 1**).

Introduction of a 2-pyridyl radical on the external nitrogen atom (**5d**, **6d**) resulted in the appearance of inhibitory activity against all three esterases with preferential inhibition of BChE. Iodine-containing compound **6d** had a higher inhibitory potency toward BChE: IC_{50} = 2.74 ± 0.25 μM than the corresponding bromine derivative (**5d**): IC_{50} = 63 ± 6 μM, while AChE and CaE were weakly inhibited by these compounds.

Insertion of a benzyl group in the starting template (**5a**, **6a**) resulted in a noticeable inhibitory activity toward BChE and CaE: compounds (**5b**, **6b**). Because the benzyl derivatives (**5b**, **6b**) were active against two enzymes of interest, BChE and CaE, they were selected for further modification.

Introduction of a second benzyl radical in the molecules (**5b**, **6b**) produced compounds (**5e**, **6e**) that inhibited BChE and CaE in the absence of anti-AChE activity. Therefore, a further search for selective and potent inhibitors of esterases was carried out among *N*,*N*-disubstituted 2-aminothiazolines.

Changing one of the benzyl radicals in (**5e**, **6e**) to 3-pyridylmethyl (**5l**, **6l**, **5m**, **6m**) led to enhancement of inhibitory activity and selectivity against BChE, which was stronger for 4-Cl substituted (**6l**) (IC_{50} = 2.47 ± 0.22 μM) than for the 2-Cl compound (**6m**) (IC_{50} = 21 ± 1 μM). The iodinated analogue (**6l**) was significantly more active than the brominated one (**5l**) (IC_{50} = 30 ± 1 μM). All 3-pyridylmethyl-containing compounds (**5l**, **6l**, **5m**, **6m**) were weak CaE inhibitors and did not have anti-AChE activity.

Further modifications were directed to the introduction of various substituents (alkyl, methoxy, hydroxyl, fluorine, chlorine) in the aryl moiety of one of the two dibenzyl fragments: compounds (**5f-i**, **6f-i**).

Introduction of a para-methoxy group (**5i**, **6i**) significantly increased the inhibitory activity and selectivity of the compounds against CaE: IC_{50} = 4.90 ± 0.45 μM (**5i**) and 4.66 ± 0.21 μM (**6i**), while BChE was inhibited weakly by these compounds (IC_{50} = 34 ± 3 μM (**5i**) and 25 ± 1 μM (**6i**)).

The presence of an isopropyl radical in the para-position (**5g**, **6g**) further enhanced activity against CaE: IC_{50} = 2.55 ± 0.23 μM (**5g**) and 2.13 ± 0.19 μM (**6g**). Moreover, in comparison to the bromine-substituted **5g**, the iodine-containing compound **6g** also exhibited relatively strong inhibitory activity against BChE: IC_{50} = 4.14 ± 0.39 μM.

Benzyl-(4-tert-butyl-benzyl)-(5-halogenomethyl-4,5-dihydro-thiazol-2-yl)-amines (**5h**, **6h**) exhibited the highest inhibitory activity against BChE and CaE. These compounds contain a *tert*-Bu group at the para-position of the benzene ring. IC_{50} values for BChE inhibition by compounds **5h** and **6h** were 2.34 ± 0.21 μM and 0.77 ± 0.07 μM, respectively. For CaE inhibition, IC_{50} values were 0.32 ± 0.03 μM (**5h)** and 0.22 ± 0.02 μM (**6h**). Compounds (**5f-i**, **6f-i**) did not inhibit AChE.

Thus, analysis of the IC_{50} values of the synthesized *N*,*N*-disubstituted 2-aminothiazolines presented in Table 1 shows that pyridine-containing compounds **5d**, **6d** and **5l**, **6l** are more selective toward BChE. Modification of the aryl moiety of one of the two dibenzyl fragments resulted in compounds (**5f-i**, **6f-i**) which did not have anti-AChE activity. Depending on the structure of the substituents at the outside nitrogen atom of *N*,*N*-disubstituted 2-aminothiazolines, the compounds exhibited preferential inhibitor activity toward CaE (compounds with a para-OMe substituent **5i**, **6i**) or both esterases. Iodine derivatives in all

cases were more effective BChE inhibitors than bromine derivatives, while there was no influence of the halogen type on CaE inhibition.

2.3. Kinetic studies of BChE and CaE inhibition.

The 9 most active compounds (**6d, 5g-i, 6g-i, 5l-6l)** toward BChE and CaE (**Table 2**) were selected for inhibition kinetics studies. Lineweaver-Burk plots -- double reciprocal plots of Michaelis-Menten parameters -- were used to evaluate the type of inhibition.

Table 2
Inhibition constants of the active *N,N*-disubstituted 2-aminothiazolines toward BChE and CaE[a].

Compounds	Enzymes			
	BChE (Equine serum)		CaE (Porcine liver)	
	K_i (μM)	αK_i (μM)	K_i (μM)	αK_i (μM)
6d		1.53 ± 0.15	nd	nd
5g	nd	nd		3.54 ± 0.34
6g	1.34 ± 0.12	7.56 ± 0.15		2.09 ± 0.19
5h	0.62 ± 0.05			0.44 ± 0.02
6h	0.27 ± 0.02	1.20 ± 0.11		0.40 ± 0.03
5i	nd	nd		7.37 ± 0.67
6i	nd	nd		7.81 ± 0.25
5l	9.51 ± 0.92	19.90 ± 1.93	nd	nd
6l	0.67 ± 0.07	3.60 ± 0.34	nd	nd

[a] Values for K_i (competitive inhibition constant) and αK_i (non-competitive inhibition constant) were determined from analyses of slopes of 1/V versus 1/S at various inhibitor concentrations. Values (means ± SEM) are from at least three separate experiments.

nd = not determined.

As seen from IC_{50} values (**Table 1**), para-tert-butyl containing compounds **5h** (Br derivative) and **6h** (I derivative) were the most potent inhibitors of both BChE and CaE. Graphical analysis of steady-state inhibition kinetics data for compounds **5h** and **6h** against BChE are shown in **Fig. 3**. For compound **5h**, raising the apparent K_m of the enzyme for the substrate did not affect V_{max}, which is consistent with competitive inhibition (**Fig. 3A**). The derived inhibition K_i was 0.62 ± 0.05 μM. In contrast, binding of **6h** to BChE changed both V_{max} and K_m values, consistent with mixed-type inhibition (**Fig. 3B**). The K_i for **6h** was 0.27

± 0.02 µM (competitive component) and αK_i was 1.20 ± 0.11 µM (noncompetitive component). Thus, replacement of Br (**5h)** with I (**6h)** led to a change of mechanism for BChE inhibition from competitive to mixed and slightly improved the inhibitory potency.

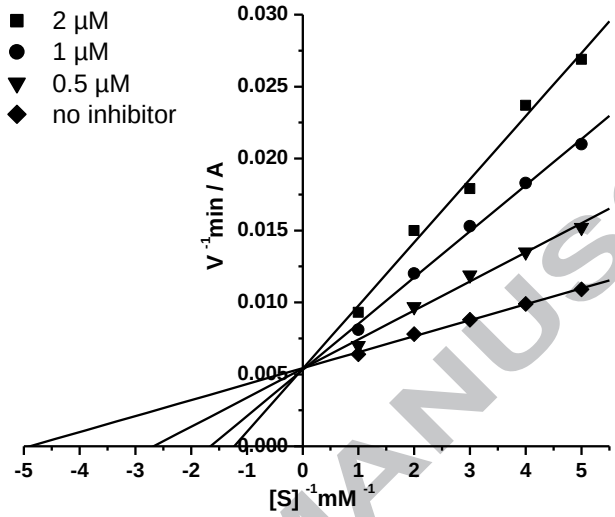

A

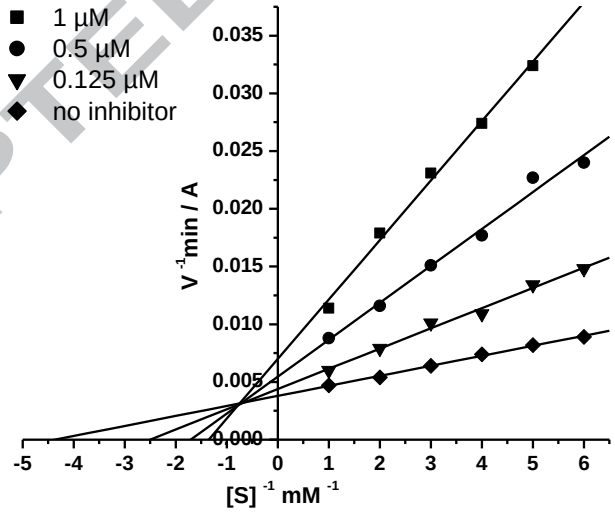

B

Figure 3. Steady state inhibition of BChE by compounds **5h** (**A**) and **6h** (**B**). Lineweaver-Burk reciprocal plots of initial velocity and substrate concentrations in the presence of inhibitors **5h, 6h** (three concentrations) and their absence are presented. Plot **A** shows competitive inhibition and plot **B** shows mixed-type inhibition.

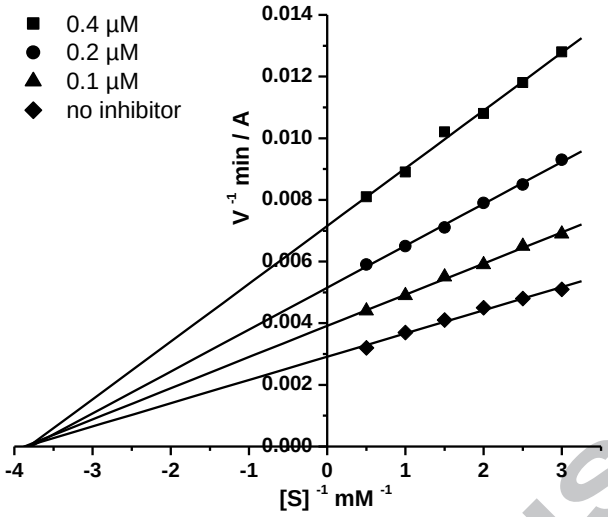

A

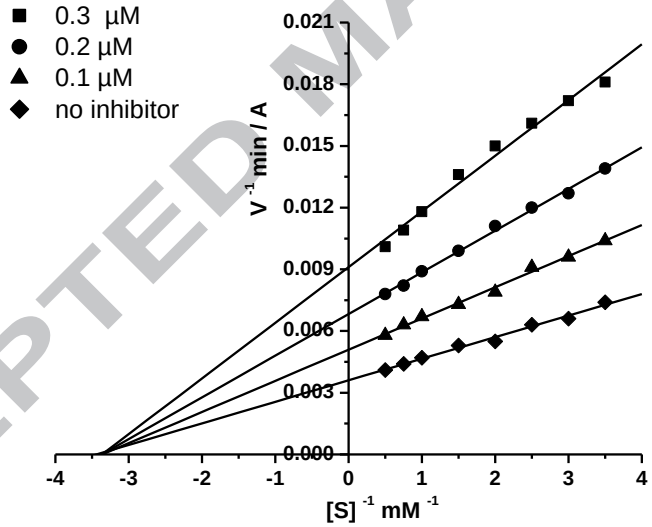

B

Figure 4. Steady state inhibition of CaE by compounds **5h** (**A**) and **6h** (**B**). Lineweaver-Burk reciprocal plots of initial velocity and substrate concentrations in the presence of inhibitors **5h, 6h** (three concentrations) and their absence are presented. Plots **A** and **B** show non-competitive inhibition.

Compounds **5h** and **6h** were also the most effective CaE inhibitors. Moreover, as shown in **Fig. 4**, increasing inhibitor concentrations resulted in a decrease in V_{max} while K_m remained unchanged. This is typical of non-competitive inhibition. Both compounds had

virtually identical inhibitor constants: 0.44 ± 0.02 μM (**5h**) and 0.40 ± 0.03 μM (**6h**). Thus, in contrast to BChE inhibition, replacement of Br with I in the inhibitor did not change the mechanism or efficiency of CaE inhibition.

Compounds with an iso-Pr group in the para-position (**5g**, **6g)** demonstrated similar inhibition kinetics (plots not shown) as **5h** and **6h** while being less potent against both BChE and CaE. The iodinated derivative **6g** was more potent than the brominated compound **5g** against BChE; it was a mixed-type inhibitor with K_i = 1.34±0.12 μM and αK_i=7.56±0.15 μM.

CaE inhibition by para-iso-Pr substituted compounds **5g** and **6g** was described by non-competitive kinetics, and the inhibition constants were close: αK_i = 3.54±0.34 μM (**5g**) and 2.09±0.19 μM (**6g**). Thus, the type of halogen (Br or I) had no effect on inhibition mechanism and little or no effect on inhibitory potency.

Para-OMe containing compounds **5i** and **6i** demonstrated selectivity toward CaE in comparison to BChE. Inhibition of CaE occurred by a non-competitive mechanism (unchanged K_m and decreased V_{max} with increasing inhibitor concentrations). The Br and I derivatives had overlapping inhibitor constants: αK_i = 7.37 ± 0.67 and 7.81 ± 0.25 μM, respectively.

Pyridine-containing compounds (**6d, 5l, 6l**) in general showed selectivity toward BChE in comparison to CaE. Thus, the active compound containing a 2-pyridinyl fragment **6d** (I derivative) inhibited BChE according to a non-competitive mechanism (K_m = constant, V_{max} = decreased with increasing inhibitor concentrations); αK_i=1.53 ± 0.15 μM.

3-Pyridinyl-containing compounds **5l** (Br-derivative) and **6l** (I-derivative) displayed mixed-type inhibition toward BChE (decreasing V_{max} and increasing K_m with increasing inhibitor concentrations). The I-derivative **6l** was more potent (K_i = 0.67 ± 0.07, αK_i = 3.60 ± 0.34 μM) than the Br-derivative **5l** (K_i = 9.51 ± 0.92 μM, αK_i = 19.90 ± 1.93 μM).

Thus, inhibition kinetics of *N,N*-disubstituted 2-aminothiazolines against BChE and CaE demonstrated that CaE inhibition was in all cases non-competitive, whereas BChE inhibition was competitive, mixed, or non-competitive depending on the structural features of the compound.

To gain insight into the various inhibitory mechanisms and differences in inhibitor potency and selectivity, molecular docking simulations were performed.

2.4. Molecular modeling studies.

To help explain the different activities of the target compounds and clarify their interaction mode in the active sites of BChE and CaE, molecular docking simulations were performed for compounds **5h, 6h, 5l, 6l, 5i, 6i, 5e, 6e, 5g, 6g, 5d, 6d, 6m** using Autodock 4.2 software. The docking results for compounds **5e, 6e, 5g, 6g, 5d, 6d,** and **6l-6m** comparison are presented in the supplementary material (**Fig. S1-S4**).

The modeling results showed that the best docked positions of the studied compounds inside BChE were within the active site, at the bottom of the gorge, in close proximity to the catalytic triad residues. In contrast, the best binding positions for CaE were clustered rather far from the active site, at the top of the gorge, and the ligands were surrounded by several leucines, isoleucines and methionines. This difference between BChE and CaE in the location of the inhibitor inside the gorge was observed for the most of studied compounds.

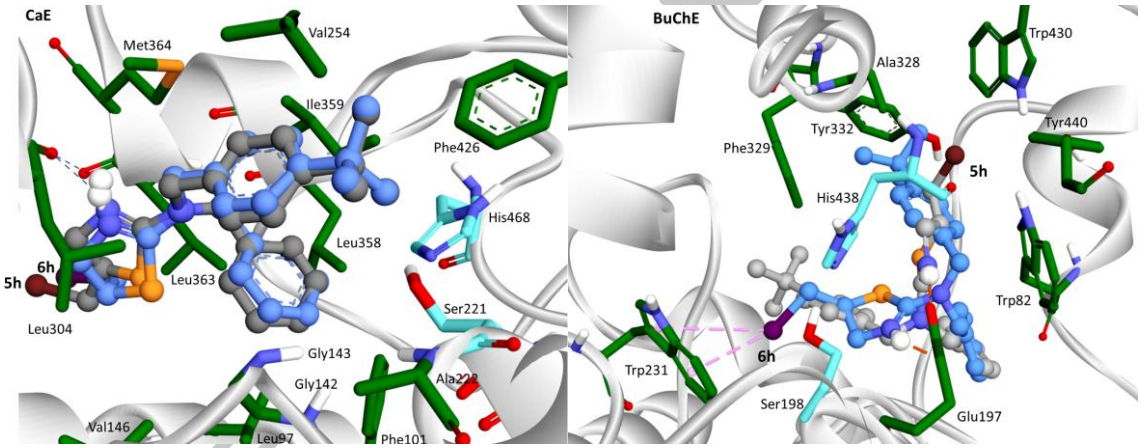

A **B**

Figure 5. Binding positions of compounds **5h** (carbon atoms are colored grey) and **6h** (carbon atoms are colored blue) inside the gorge of human CaE (**A**) and BChE (**B**). Carbon atoms of the enzyme residues side chains are colored green and the catalytic residues are depicted in cyan.

Tert-Bu-containing compounds **5h** and **6h** were the most active inhibitors of both BChE and CaE. Both compounds were located rather far from the active site of CaE, at the top of the gorge (**Fig. 5A**). Positions of the Br-analogue **5h** and I-analogue **6h** inside CaE were very similar; no significant difference was observed. This is because their halogen atoms emerge from the mouth of the gorge and do not interact with protein atoms. The modeling results agree with the experimentally observed non-competitive mechanism of CaE inhibition by Br- and I-analogues, **5h** and **6h**, and their equivalent inhibitor activity against CaE.

The best docked positions of **5h** and **6h** inside BChE were within the active site (**Fig. 5B**), at the bottom of the gorge, in close proximity to the catalytic residues. The main contributors to binding of both **5h** and **6h** with the BChE active site were electrostatic interactions and hydrogen bonds of the positively charged thiazoline fragment (amidine group) and the negatively charged carboxylic group of Glu197. Additionally, **6h** had C-I…π interactions with Trp231. Its Br-containing analogue **5h** occupied a mirror-image position, but with the halogen atom too far from Trp430 and Trp82 to interact with their aromatic rings. This difference in halogen interactions explains the higher inhibitory activity of the I-derivative **6h** toward BChE and the different mechanisms of BChE inhibition by the Br- and I-derivatives.

In contrast to CaE, the active site of BChE contains numerous aromatic side chains; this difference furnishes a possible reason for the influence exerted by the halogen atom on the binding of inhibitors to BChE. Most of I-derivatives tended to interact with aromatic rings, in particular, the indole ring of tryptophan residues. This observation corresponds well with recently reported findings that halogens, in particular I, form rather strong halogen bonds, including C-I…π interactions, comparable with strong hydrogen bonds [40, 41]. The indole rings of Trp82 and Trp231 are aligned parallel to the BChE gorge wall, while the phenyl rings of Phe329 and Phe398 are oriented in a more perpendicular fashion. This geometrical arrangement favors interactions of the iodine atoms with the tryptophan residues.

Docking results for compounds with an *iso*-Pr group in the para-position (**5g**, **6g**) were similar to those observed for the tert-Bu compounds **5h** and **6h** (see supplementary data, **Fig. S2**), again in agreement with the kinetics studies.

The presence of aromatic groups in the active site of BChE also ensures higher binding affinities to compounds containing a pyridine ring. The situation is quite different for CaE, which lacks aromatic residues in the gorge, particularly at the entrance, where most of the CaE inhibitors bind. The lip of the CaE gorge is mainly lined with methionines and other aliphatic residues.

Compounds **5l** and **6l** containing a 3-pyridinyl ring were more effective inhibitors of BChE than CaE. These are mixed-type BChE inhibitors, and the I-derivative **6l** is more active than the Br-derivative **5l**. These compounds bind with BChE very tightly, fully occupying its active site (**Fig. 6A,B**). In each compound, the protonated thiazoline fragment forms a strong hydrogen bond with Glu197. However, the arrangement of other molecular fragments differs between the two compounds. In **5l**, the pyridine ring is oriented with its nitrogen atom in the oxyanion hole, where it forms hydrogen bonds with the peptide bond nitrogen atoms of Gly117 and Ala199. For **6l**, the p-Cl-phenyl ring is parallel to Trp82 and thus has strong π-π

interactions (**Fig. 6A**). The Br atom of **5l** is inserted into a cavity formed by the side chains of Leu125 and Thr120 and the backbone chains of Gly121 and Trp82 (**Fig. 6B**). However, the I atom of **6l** has a larger van der Waals radius than Br and cannot fit into this cavity, thus creating the difference in orientation between these two similar ligands.

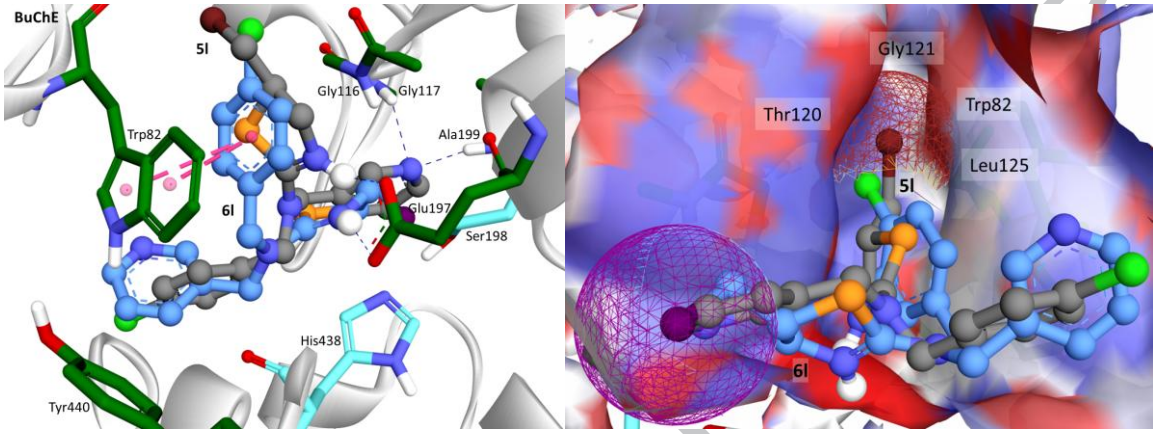

A **B**

Figure 6. Binding positions of compounds **5l** (carbon atoms are colored grey) and **6l** (carbon atoms are colored blue) in the active site of BChE. (**A**) and (**B**) are views from different vantage points. In panel (**A**) carbon atoms of BChE residues side chains are colored green and the catalytic residues are rendered in cyan; in panel (**B**) BChE solvent accessible surface and van der Waals spheres of the inhibitor halogen atoms are shown.

Compounds with an OMe group in the para-position of one of the two dibenzyl fragments (**5i** and **6i**) are more selective for CaE than BChE. The position of these two compounds in CaE is close to the active site, with the methoxy group located near Ser221 in an orientation favorable for formation of hydrogen bonds both with the catalytic serine and oxyanion hole (**Fig. 7A**). Halogen atoms are oriented towards the mouth of the gorge and therefore have no influence on binding position. In the case of BChE, the orientation of these inhibitors is determined by interaction of the halogen atoms with Trp231 (**Fig. 7B**), and binding is otherwise highly favorable (**6i** has π-π interactions with Trp82 and forms a hydrogen bond between the OMe group and Tyr128, whereas the positively charged thiazoline group of **5i** interacts with Glu197). Given that the molecular docking results reveal favorable interactions of these compounds both the active sites of both CaE and BChE, the reason for the experimentally determined selectivity of these compounds for CaE must lie elsewhere, such as differences in transport through the gorge to the active site of the enzymes. Future studies

using molecular dynamics simulations might be used to explore the plausibility of this explanation.

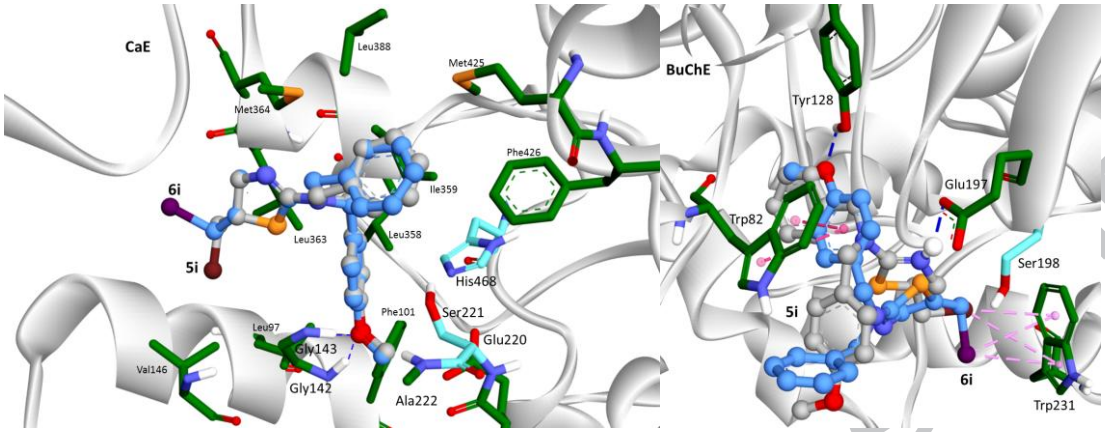

A **B**

Figure 7. Binding positions of compounds **5i** (carbon atoms are colored grey) and **6i** (carbon atoms are colored blue) inside the gorge of human CaE (**A**) and BChE (**B**). Carbon atoms of the enzyme residues side chains are colored green and the catalytic residues are depicted in cyan.

2.5. Cytotoxicity studies

To investigate the effect of the test compounds on cell viability, cytotoxicity studies for these compounds were performed on human fetal mesenchymal stem cells using the MTT/formazan assay. At the limit of solubility of these compounds (less than 30 µM), none of the tested compounds resulted in a significant decrease in cell viability (data not shown).

3. Conclusions

In summary, a novel series of *N*,*N*-disubstituted 2-aminothiazolines has been designed, synthesized and evaluated as AChE, BChE, and CaE inhibitors. The results demonstrate that the tested compounds do not inhibit AChE; accordingly, they would be expected not to cause unwanted cholinergic side effects if they were employed, e.g., as co-drugs for ester-containing pharmacological agents. The relative selectivity of the most active compounds toward BChE and CaE is summarized in **Fig. 8**. Whereas the compounds did not inhibit AChE, the level of anti-BChE and anti-CaE activity depended on the structure of the compounds. Pyridine-containing compounds were more selective toward BChE and compounds with a *para*-OMe substituent in one of the two dibenzyl fragments were more selective toward CaE. Iodinated derivatives were more effective BChE inhibitors than

brominated ones, while there was no influence of the halogen type on CaE inhibition. The most potent inhibitors of BChE and CaE were the benzyl-(4-tert-butyl-benzyl)-(5-halogenomethyl-4,5-dihydro-thiazol-2-yl)-amines. IC_{50} values for BChE inhibition by **5h (**X=Br**)** and **6h** (X=I) were 2.34 ± 0.21 µM and 0.77 ± 0.07 µM, respectively. For CaE inhibition, IC_{50} values were 0.32 ± 0.03 µM (**5h)** and 0.22 ± 0.02 µM (**6h**).

The kinetic studies performed for the most active compounds demonstrated that all studied compounds acted as non-competitive CaE inhibitors and exhibited different mechanisms (competitive, non-competitive, or mixed-type) of BChE inhibition depending on the structural features of the compound. Docking simulations showed the best docked positions of the compounds inside BChE were within the active site, at the bottom of the gorge, in close proximity to the catalytic residues. In contrast, the best binding positions for CaE were clustered rather far from the active site, at the top of the gorge. The docking results help explain differences in the kinetic mechanisms and inhibitor activity of the tested compounds. A cytotoxicity test using the MTT assay showed that within solubility limits (< 30 µM), none of the tested compounds significantly affected viability of human fetal mesenchymal stem cells.

Overall, the results indicated that members of a novel series of *N,N*-disubstituted 2-aminothiazolines have the potential to be good candidates for BChE and CaE inhibitors for potential medicinal applications.

4. Experimental section

4.1. Chemistry

All solvents, chemicals, and reagents were obtained commercially and used without purification. ^{1}H NMR (200 MHz) spectra were recorded on a Bruker CXP-200 NMR spectrometer using $CDCl_3$, DMSO-D_6, acetone-d_6, CD_3OD, CD_3CN, or D_2O as solvents with tetramethylsilane as an internal standard. Chemical shifts, d, are given in parts per million (ppm), and spin multiplicities are given as s (singlet), br s (broad singlet), d (doublet), t (triplet), q (quartet) or m (multiplet). Coupling constants, J, are expressed in hertz (Hz). Melting points were recorded on a Boetius hot-plate apparatus and are uncorrected. Yields refer to isolated pure products and were not maximized. CHN analysis was performed on a CHN elemental analyzer vario MICRO cube (elementar GmbH). The MS spectra were recorded using a Thermo Fisher Exactive instrument with an Orbitrap mass analyzer.

4.2. Synthesis of compounds

4.2.1. A general procedure for the synthesis of compounds

A solution of allylisothiocyanate **1** (0.99 g, 0.01 M) in 20 ml of diethyl ether (ether) was added dropwise to a solution of amine **2** (0.01 M) in 20 ml of ether with intensive stirring. The reaction mixture was stirred for 2–5 h at room temperature. The thiourea precipitate **3** was filtered, dried and dissolved in 20 ml methanol and a solution of halogen (0.01 M) in 5 ml methanol was added dropwise. The reaction mixture was stirred 24 h at room temperature, evaporated to 1/3 volume and diluted with 20 ml of ether. The precipitate was filtered, recrystallized from isopropanol, and the hydrohalogen 5-halomethyl-2-aminothiazolines **5, 6** were obtained with high yields as noted below.

*4.2.2. 5-Bromomethyl-4,5-dihydro-thiazol-2-ylamine hydrobromide (**5a**)*

Yield: 86%; mp: 145-147 °C;

^{1}H NMR (200 MHz, D_2O): δ = 3.74 (dd, J = 2.1, 6.7 Hz, 2H, NCH_2), 4.07 (dd, J = 2.1, 5.1 Hz, 2H, $BrCH_2$), 4.45 (m, 1H, CHS);

EI-MS (m/z): 277.0 ($M + H^+$).

Anal. Calcd. for $C_4H_8Br_2N_2S$: C 17.41; H 2.92; N 10.15. Found: C 17.48; H 2.97; N 10.10.

*4.2.3. 5-Iodomethyl-4,5-dihydro-thiazol-2-ylamine hydroiodide (**6a**).*

Yield: 82%; mp: 127-129 °C;

^{1}H NMR (200 MHz, DMSO-d_6): 3.62 (m, 2H, NCH_2), 3.80 (dd, J = 3.7, 12.0 Hz, 1H, IC<u>H</u>H), 4.00 (dd, J = 7.3, 12.0 Hz, 1H, ICH<u>H</u>), 4.37 (m, 1H, CHS), 9.30 (br s, 3H, NH_3);

EI-MS (m/z): 371 ($M + H^+$).

Anal. Calcd. for $C_4H_8I_2N_2S$: C 12.99; H 2.18; N 7.57. Found: C 13.09; H 2.11; N 7.63

*4.2.4. Benzyl-(5-bromomethyl-4,5-dihydro-thiazol-2-yl)-amine hydrobromide (**5b**)*

Yield: 87%; mp: 80-82 °C;

^{1}H NMR (200 MHz, $CDCl_3$): δ = 3.55 (d, J = 7.3 Hz, 2H, $PhCH_2$), 4.07 (m, 2H, N<u>C</u>H_2CHS), 4.20 (m, 1H, BrC<u>H</u>H), 4.49 (m, 2H, ICHH, CHS), 7.33 (m, 5H, H_{arom}), 10.19 (br s, 1H, NH), 10.61 (br s, 1H, NH);

EI-MS (m/z): 367 ($M + H^+$).

Anal. Calcd. for $C_{11}H_{14}Br_2N_2S$: C 36.09; H 3.85; N 7.65. Found: C 36.01; H 3.88; N 7.72.

*4.2.5. Benzyl-(5-iodomethyl-4,5-dihydro-thiazol-2-yl)-amine hydroiodide (**6b**)*

Yield: 77%; mp: 173-175 °C;

^{1}H NMR (200 MHz, DMSO-d_6): 3.39 (d, J = 7.0 Hz, 2H, $PhCH_2$), 3.87 (m, 2H, N<u>C</u>H_2CHS), 4.01 (m, 1H, BrC<u>H</u>H), 4.28 (m, 2H, ICHH, CHS), 7.01 (m, 5H, H_{arom}), 9.71 (br s, 1H, NH), 10.11 (br s, 1H, NH);

EI-MS (m/z): 461 ($M + H^+$).

Anal. Calcd. for $C_{11}H_{14}I_2N_2S$: C 28.71; H 3.07; N 6.09. Found: C 28.78; H 3.09; N 6.05.

*4.2.6. (5-Bromomethyl-4,5-dihydro-thiazol-2-yl)-phenyl-amine hydrobromide (**5c**)*

Yield: 86%; mp: 150-152 °C;

^{1}H NMR (200 MHz, DMSO-d_6): δ = 3.88 (dd, J = 2.9, 9.3 Hz, 1H, BrC<u>H</u>H), 3.91 (d, J = 6.4 Hz, 2H, NCH_2), 4.11 (dd, J = 7.6, 12.0 Hz, 1H, BrCH<u>H</u>), 7.45 (m, 5H, H_{arom}), 11.1 (br s, 1H, NH);

EI-MS (m/z): 353 ($M + H^+$).

Anal. Calcd. for $C_{10}H_{12}Br_2N_2S$: C 34.11; H 3.44; N 7.96. Found: C 34.21; H 3.48; N 8.01.

*4.2.7. (5-Iodomethyl-4,5-dihydro-thiazol-2-yl)-phenyl-amine hydroiodide (**6c**)*

Yield: 85%; mp: 135-137 °C;

^{1}H NMR (200 MHz, CD_3OD): 3.75 (d, J = 7.0 Hz, 2H, NC<u>H$_2$</u>CHS), 4.05 (dd, J = 3.5, 12.1 Hz, 1H, IC<u>H</u>H), 4.24 (dd, J = 7.4, 12.1 Hz, 1H, ICH<u>H</u>), 4.55 (m, 1H, CHS), 7.50 (m, 5H, H_{arom});

EI-MS (m/z): 447 ($M + H^+$).

Anal. Calcd. for $C_{10}H_{12}I_2N_2S$: C 26.93; H 2.71; N 6.28. Found: C 26.99; H 2.74; N 6.21.

*4.2.8. (5-Bromomethyl-4,5-dihydro-thiazol-2-yl)-pyridin-2-yl-amine hydrobromide (**5d**)*

Yield: 83%; mp: 156-158 °C;

^{1}H NMR (200 MHz, DMSO-d_6): δ = 3.84 (m, 2H, NCH_2), 4.16 (m, 2H, $BrCH_2$), 4.43 (m, 1H, CHS), 7.26 (dd, J = 5.1, 6.9 Hz, 1H, H_{arom}), 7.42 (d, J = 8.3 Hz, 1H, H_{arom}), 7.92 (m, 1H, H_{arom}), 8.41 (d, J = 3.7 Hz, 1H, H_{arom});

EI-MS (m/z): 354 ($M + H^+$).

Anal. Calcd. for $C_9H_{11}Br_2N_3S$: C 30.62; H 3.14; N 11.90. Found: C 30.68; H 3.19; N 11.95.

*4.2.9. (5-Iodomethyl-4,5-dihydro-thiazol-2-yl)-pyridin-2-yl-amine hydroiodide (**6d**)*

Yield: 76%; mp: 137-139 °C;

^{1}H NMR (200 MHz, DMSO-d_6): δ = 3.73 (d, J = 7.1 Hz, 2H, NC<u>H$_2$</u>CHS), 4.06 (dd, J = 3.5, 12.0 Hz, 1H, IC<u>H</u>H), 4.22 (dd, J = 7.4, 12.0 Hz, 1H, ICH<u>H</u>), 4.53 (m, 1H, CHS), 7.27 (m, 1H, H_{arom}), 7.41 (d, J = 8.2 Hz, 1H, H_{arom}), 7.95 (m, 1H, H_{arom}), 8.38 (m, 1H, H_{arom});

EI-MS (m/z): 448 ($M + H^+$).

Anal. Calcd. for $C_9H_{11}I_2N_3S$: C 24.18; H 2.48; N 9.40. Found: C 24.24; H 2.53; N 9.33.

*4.2.10. Benzyl-(5-bromomethyl-4,5-dihydro-thiazol-2-yl)-(4-fluoro-benzyl)-amine hydrobromide (**5e**)*

Yield: 77%; mp: 178-180 °C;

^{1}H NMR (200 MHz, DMSO-d_6): δ = 3.88 (d, J = 6.4 Hz, 2H, NC$\underline{H}_2$CHS), 4.05 (dd, J = 3.2, 12.5 Hz, 1H, BrC$\underline{H}$H), 4.20 (dd, J = 7.3, 12.5 Hz, 1H, BrCH$\underline{H}$), 4.57 (m, 1H, CHS), 4.71 (s, 4H, CH_2NCH_2), 7.31 (m, 10H, H_{arom});

EI-MS (m/z): 457 ($M + H^+$).

Anal. Calcd. for $C_{18}H_{20}Br_2N_2S$: C 47.39; H 4.42; N 6.14. Found: C 47.47; H 4.47; N 6.08.

*4.2.11. Dibenzyl-(5-iodomethyl-4,5-dihydro-thiazol-2-yl)-amine hydroiodide (**6e**)*

Yield: 81%; mp: 165-167 °C;

^{1}H NMR (200 MHz, DMSO-d_6): δ = 3.68 (d, J = 6.4 Hz, 2H, NC$\underline{H}_2$CHS), 4.05 (dd, J = 3.2, 12.0 Hz, 1H, BrC$\underline{H}$H), 4.21 (dd, J = 7.2, 12.0 Hz, 1H, BrCH$\underline{H}$), 4.48 (m, 1H, CHS), 4.71 (s, 4H, CH_2NCH_2), 7.38 (m, 10H, H_{arom}), 10.50 (br s, 1H, NH);

EI-MS (m/z): 551 ($M + H^+$).

Anal. Calcd. for $C_{18}H_{20}I_2N_2S$: C 39.29; H 3.66; N 5.09. Found: C 39.33; H 3.66; N 5.13.

*4.2.12. Benzyl-(4-fluoro-benzyl)-(5-iodomethyl-4,5-dihydro-thiazol-2-yl)-amine hydrobromide (**5f**)*

Yield: 78%; mph: 178-180 °C;

^{1}H NMR (200 MHz, $CDCl_3$): δ = 3.72 (d, J = 6.3 Hz, 2H, NC$\underline{H}_2$CHS), 4.33 (m, 2H, $BrCH_2$), 4.43 (m, 1H, CHS), 4.50 (c, 2H, C$\underline{H}_2$NCH$_2$), 5.10 (c, 2H, CH$_2$NC$\underline{H}_2$), 7.09 (m, 4H, H_{arom}), 7.38 (m, 5H, H_{arom}), 11.59 (c, 1H, NH);

EI-MS (m/z): 475 ($M + H^+$).

Anal. Calcd. for $C_{18}H_{19}Br_2FN_2S$: C 45.59; H 4.04; N 5.91. Found: C 45.51; H 4.11; N 5.88.

*4.2.13. Benzyl-(4-fluoro-benzyl)-(5-iodomethyl-4,5-dihydro-thiazol-2-yl)-amine hydroiodide (**6f**)*

Yield: 88%; mp: 163-165 °C;

^{1}H NMR (200 MHz, CD_3CN): δ = 3.72 (m, 2H, NC$\underline{H}_2$CHS), 4.11 (m, 2H, ICH_2), 4.50 (m, 1H, CHS), 4.73 (m, 4H, CH_2NCH_2), 7.04 (m, 2H, H_{arom}), 7.20 (m, 2H, H_{arom}), 7.35 (m, 2H, H_{arom}), 7.47 (m, 3H, H_{arom}), 8.90 (br s, 1H, HI);

EI-MS (m/z): 569($M + H^+$).

Anal. Calcd. for $C_{18}H_{19}FI_2N_2S$: C 38.05; H 3.37; N 4.93. Found: $C_{18}H_{19}FI_2N_2S$: C 38.00; H 3.33; N 4.96

*4.2.14. Benzyl-(5-bromomethyl-4,5-dihydro-thiazol-2-yl)-(4-isopropyl-benzyl)-amine hydrobromide (**5g**)*

Yield: 82%; mp: 118-120 °C;

^{1}H NMR (200 MHz, $CDCl_3$): δ = 1.25 (d, J = 6.8 Hz, 6H, $CH(C\underline{H}_3)_2$), 2.92 (m, 1H, $C\underline{H}(CH_3)_2$), 3.53 (d, J = 6.0 Hz, 2H, $NC\underline{H}_2CHS$), 4.34 (m, 3H, CHS, $BrCH_2$), 4.55 (br. s, 2H, $C\underline{H}_2NCH_2$), 5.02 (br. s, 2H, $CH_2NC\underline{H}_2$), 7.25 (m, 6H, H_{arom}) , 7.40 (m, 3H, H_{arom});

EI-MS (m/z): 499 ($M + H^+$).

Anal. Calcd. for $C_{21}H_{26}Br_2N_2S$: C 50.62; H 5.26; N 5.62. Found: C 50.60; H 5.21; N 5.64.

*4.2.15. Benzyl-(4-isopropyl-benzyl)-(5-iodomethyl-4,5-dihydro-thiazol-2-yl)-amine hydroiodide (**6g**)*

Yield: 84%; mp: 143-145 °C;

^{1}H NMR (200 MHz, $CDCl_3$): δ = 1.24 (d, J = 6.8 Hz, 6H, $CH(C\underline{H}_3)_2$), 2.92 (m, 1H, $C\underline{H}(CH_3)_2$), 3.53 (d, J = 5.9 Hz, 2H, $NC\underline{H}_2CHS$), 4.27 (m, 2H, ICH_2), 4.45 (m, 1H, CHS), 4.77 (m, 4H, CH_2NCH_2), 7.21 (m, 6H, H_{arom}), 7.39 (m, 3H, H_{arom});

EI-MS (m/z): 593($M + H^+$).

Anal. Calcd. for $C_{21}H_{26}I_2N_2S$: C 42.58; H 4.42; N 4.73. Found: C 42.52; H 4.40; N 4.77.

*4.2.16. Benzyl-(5-bromomethyl-4,5-dihydro-thiazol-2-yl)-(4-tert-butyl-benzyl)-amine hydrobromide (**5h**)*

Yield: 87%; mp: 138-140 °C;

^{1}H NMR (200 MHz, DMSO-d_6): δ = 1.29 (s, 9H, $C(CH_3)_3$), 3.89 (d, J = 6.4 Hz, 2H, $NC\underline{H}_2CHS$), 4.05 (dd, J = 3.2, 12.0 Hz, 1H, $BrC\underline{H}H$), 4.21 (dd, J = 7.3, 12.0 Hz, 1H, $BrCH\underline{H}$), 4.58 (m, 1H, CHS), 4.64 (br. s, 4H, CH_2NCH_2), 6.87 (d, J = 8.8 Hz, 2H, H_{arom}), 7.27 (m, 7H, H_{arom});

EI-MS (m/z): 513 ($M + H^+$).

Anal. Calcd. for $C_{22}H_{28}Br_2N_2S$: C 51.57; H 5.51; N 5.47. Found: C 51.68; H 5.57; N 5.41.

*4.2.17. Benzyl-(4-tert-butyl-benzyl)-(5-iodomethyl-4,5-dihydro-thiazol-2-yl)-amine hydroiodide (**6h**)*

Yield: 83%; mp: 161-163 °C;

^{1}H NMR (200 MHz, $CDCl_3$): δ = 1.30 (s, 9H, $C(CH_3)_3$), 3.53 (d, J = 7.1 Hz, 2H, $NC\underline{H}_2CHS$), 4.24 (m, 2H, ICH_2), 4.50 (m, 1H, CHS), 4.53 (br s, 2H, $C\underline{H}_2NCH_2$), 5.05 (br s, 2H, $CH_2NC\underline{H}_2$), 7.15 (m, 4H, H_{arom}), 7.45 (m, 5H, H_{arom}), 10.40 (br s, 1H, HI);

EI-MS (m/z): 607 ($M + H^+$).

Anal. Calcd. for $C_{22}H_{28}I_2N_2S$: C 43.58; H 4.65; N 4.62. Found: C 43.52; H 4.66; N 4.66.

*4.2.18. Benzyl-(5-bromomethyl-4,5-dihydro-thiazol-2-yl)-(4-methoxy-benzyl)-amine hydrobromide (**5i**)*

Yield: 90%; mp: 112-114 °C;

^{1}H NMR (200 MHz, DMSO-d_6): δ = 3.77 (s, 3H, OCH_3), 3.88 (m, 2H, NCH_2CHS), 4.05 (dd, J = 3.2, 12.0 Hz, 1H, $BrCHH$), 4.21 (dd, J = 7.3, 12.0 Hz, 1H, $BrCHH$), 4.64 (m, 5H, CHS, CH_2NCH_2), 6.87 (d, J = 8.8 Hz, 2H, H_{arom}), 7.27 (m, 7H, H_{arom});

EI-MS (m/z): 487 ($M + H^+$).

Anal. Calcd. for $C_{19}H_{22}Br_2N_2OS$: C 46.93; H 4.56; N 5.76. Found: C 46.99; H 4.62; N 5.70.

*4.2.19. Benzyl-(5-iodomethyl-4,5-dihydro-thiazol-2-yl)-(4-methoxy-benzyl)-amine hydroiodide (**6i**)*

Yield: 82%; mp: 150-152 °C;

^{1}H NMR (200 MHz, CD_3CN): δ = 3.68 (m, 2H, NCH_2CHS), 3.85 (s, 3H, OCH_3), 4.10 (m, 2H, ICH_2), 4.45 (m, 1H, CHS), 4.75 (m, 4H, 2x$PhCH_2$), 7.17 (d, J = 8.8 Hz, 2H, H_{arom}), 7.26 (d, J = 8.8 Hz, 2H, H_{arom}), 7.33 (m, 2H, H_{arom}), 7.45 (m, 3H, H_{arom}), 8.95 (br s, 1H, HI);

EI-MS (m/z): 581 ($M + H^+$).

Anal. Calcd. for $C_{19}H_{22}I_2N_2OS$: C 39.33; H 3.82; N 4.83. Found: C 39.31; H 3.84; N 4.85.

*4.2.20. Benzyl-(5-bromomethyl-4,5-dihydro-thiazol-2-yl)-(1-phenyl-ethyl)-amine hydrobromide (**5k**)*

Yield: 85%; mp: 167-169 °C;

^{1}H NMR (200 MHz, DMSO-d_6): δ = 1.60 (d, J = 6.5 Hz, 3H, CH_3), 3.91 (d, J = 6.5 Hz, NCH_2CHS), 4.01 (d, J = 12.0 Hz, 1H, $BrCHH$), 4.21 (dd, J = 7.5, 12.0 Hz, 1H, $BrCHH$), 4.56 (m, 2H, CHS, $PhCHH$), 4.81 (m, 1H, $PhCHH$), 5.47 (m, 1H, $CHMe$), 7.11 (m, 2H, H_{arom}), 7.28 (m, 3H, H_{arom}), 7.39 (m, 5H, H_{arom});

EI-MS (m/z): 471 ($M + H^+$).

Anal. Calcd. for $C_{19}H_{22}Br_2N_2S$: C 48.53; H 4.72; N 5.96. Found: C 48.59; H 4.772; N 6.02.

*4.2.21. Benzyl-(5-iodomethyl-4,5-dihydro-thiazol-2-yl)-(1-phenyl-ethyl)-amine hydroiodide (**6k**)*

Yield: 76%; mp: 155-157 °C.

^{1}H NMR (200 MHz, CD_3CN): δ = 1.72 (d, J = 6.8 Hz, 3H, CH_3), 3.69 (m, 2H, NCH_2CHS), 4.05 (m, 1H, $ICHH$), 4.10 (m, 1H, $ICHH$), 4.50 (m, 1H, CHS), 4.74 (m, 2H, $PhCH_2$), 5.63 (m, 1H, $CHMe$), 7.18 (m, 2H, H_{arom}), 7.43 (m, 7H, H_{arom}), 8.85 (br s, 1H, HI);

EI-MS (m/z): 565($M + H^+$).

Anal. Calcd. for $C_{19}H_{22}I_2N_2S$: C 40.44; H 3.93; N 4.96. Found: C 40.22; H 3.98; N 4.92.

*4.2.22. (5-Bromomethyl-4,5-dihydro-thiazol-2-yl)-(4-chloro-benzyl)-pyridin-3-ylmethyl-amine hydrobromide (**5l**)*

Yield: 88%; mp: 188-190 °C;

^{1}H NMR (200 MHz, DMSO-d_6): δ = 3.86 (m, 2H, NC$\underline{H}_2$CHS), 4.14 (m, 2H, BrCH_2) , 4.51 (m, 1H, CHS), 4.85 (br. s, 2H, CH_2NC$\underline{H}_2$), 5.07 (br. s, 2H, C$\underline{H}_2$NCH_2), 7.36 (m, 4H, H_{arom}), 7.88 (dd, J = 5.4, 8.4 Hz, 1H, H_{arom}), 7.83 (d, J = 8.4 Hz, 1H, H_{arom}), 8.49 (d, J = 5.4 Hz, 1H, H_{arom}), 8.91 (s, 1H, H_{arom});

EI-MS (m/z): 492 ($M + H^+$).

Anal. Calcd. for $C_{17}H_{18}Br_2ClN_3S$: C 41.59; H 3.61; N 8.62. Found: C 41.22; H 3.98; N 8.92.

*4.2.23. (4-Chloro-benzyl)-(5-iodomethyl-4,5-dihydro-thiazol-2-yl)-pyridin-3-ylmethyl-amine hydroiodide (**6l**)*

Yield: 85%; mp: 100-102 °C;

^{1}H NMR (200 MHz, DMSO-d_6): 3.47 (m, 2H, NC$\underline{H}_2$CHS), 3.69 (dd, J = 2.7, 12.2 Hz, 1H, IC$\underline{H}$H), 3.93 (dd, J = 7.1, 12.2 Hz, 1H, ICH$\underline{H}$), 4.29 (m, 1H, CHS), 4.60 (c, 2H, C$\underline{H}_2$NCH_2), 4.73 (c, 2H, CH_2NC$\underline{H}_2$), 7.19 (dd, J = 8.3, 19.0 Hz, 4H, H_{arom}), 7.74 (dd, J = 5.8, 7.8 Hz, 1H, H_{arom}), 8.16 (d, J = 7.8 Hz, 1H, H_{arom}), 8.61 (c, 1H, H_{arom}), 8.63 (d, J = 5.8 Hz, 1H, H_{arom});

EI-MS (m/z): 586 ($M + H^+$).

Anal. Calcd. for $C_{17}H_{18}ClI_2N_3S$: C 34.86; H 3.10; N 7.17. Found: C 34.91; H 3.15; N 7.11.

*4.2.24. (5-Bromomethyl-4,5-dihydro-thiazol-2-yl)-(2-chloro-benzyl)-pyridin-3-ylmethyl-amine hydrobromide (**5m**)*

Yield: 88%; mp: 173-175 °C;

^{1}H NMR (200 MHz, $CDCl_3$): 3.83 (m, 2H, NC$\underline{H}_2$CHS), 4.08 (dd, J = 3.2, 12.7 Hz, 1H, BrC$\underline{H}$H), 4.22 (dd, J = 7.3, 12.7 Hz, 1H, BrCH$\underline{H}$), 4.53 (m, 1H, CHS), 4.80 (c, 2H, C$\underline{H}_2$NCH_2), 4.86 (c, 2H, CH_2NC$\underline{H}_2$), 7.35 (m, 4H, H_{arom}), 7.41 (m, 1H, H_{arom}), 7.84 (m, 1H, H_{arom}), 8.51 (m, 1H, H_{arom});

EI-MS (m/z): 492 ($M + H^+$).

Anal. Calcd. for $C_{17}H_{18}Br_2ClN_3S$: C 41.53; H 3.69; N 8.55. C 41.44; H 3.62; N 8.59.

*4.2.25. (2-Chloro-benzyl)-(5-iodomethyl-4,5-dihydro-thiazol-2-yl)-pyridin-3-ylmethyl-amine hydroiodide (**6m**)*

Yield: 79%; mp: 180-182 °C;

^{1}H NMR (200 MHz, DMSO-d_6): 3.70 (m, 2H, NC$\underline{H}_2$CHS), 4.01 (dd, J = 2.9, 12.0 Hz, 1H, IC$\underline{H}$H), 4.23 (dd, J = 7.1, 12.0 Hz, 1H, ICH$\underline{H}$), 4.54 (m, 1H, CHS), 4.81 (c, 4H, CH_2NCH_2), 7.39 (m, 5H, H_{arom}), 7.85 (d, J = 7.3 Hz, 1H, H_{arom}), 8.54 (m, 2H, H_{arom});

EI-MS (m/z): 586 ($M + H^+$).

Anal. Calcd. for $C_{17}H_{18}ClI_2N_3S$: C 34.86; H 3.10; N 7.17. Found: C 34.80; H 3.18; N 7.22.

*4.2.26. Benzyl-(2-chloro-benzyl)-(5-iodomethyl-4,5-dihydro-thiazol-2-yl)-amine hydroiodide (**6n**)*

Yield: 74%; mp: 186-188 °C;

^{1}H NMR (200 MHz, DMSO-d_6): 3.73 (d, J = 6.8 Hz, 2H, NC$\underline{H}_2$CHS), 4.02 (dd, J = 2.9, 12.2 Hz, 1H, IC$\underline{H}$H), 4.24 (dd, J = 7.6, 12.2 Hz, 1H, ICH$\underline{H}$), 4.57 (m, 1H, CHS), 4.72 (c, 2H, C$\underline{H}_2$NCH$_2$), 4.76 (c, 2H, CH$_2$NC$\underline{H}_2$), 7.31 (m, 9H, H_{arom}), 10.55 (br. s. 1H, NH);

EI-MS (m/z): 585 ($M + H^+$).

Anal. Calcd. for $C_{18}H_{19}ClI_2N_2S$: C 36.98; H 3.28; N 4.79. Found: C 37.07; H 3.33; N 4.84.

*4.2.27. Benzyl-(3,4-dimethoxy-benzyl)-(5-iodomethyl-4,5-dihydro-thiazol-2-yl)-amine hydroiodide (**6o**)*

Yield: 81%; mp: 128-130 °C;

^{1}H NMR (200 MHz, $CDCl_3$): 3.56 (d, J = 6.8 Hz, 2H, NC$\underline{H}_2$CHS), 3.85 (c, 3H, OCH_3), 3.89 (c, 3H, OCH_3), 4.20 (dd, J = 3.9, 11.7 Hz, 1H, IC$\underline{H}$H), 4.37 (dd, J = 7.3, 11.7 Hz, 1H, ICH$\underline{H}$), 4.45 (m, 1H, CHS), 4.55 (br. s, 2H, C$\underline{H}_2$NCH$_2$), 4.92 (br. s, 2H, CH$_2$NC$\underline{H}_2$), 6.83 (m, 3H, H_{arom}), 7.23 (m, 2H, H_{arom}), 7.38 (m, 3H, H_{arom});

EI-MS (m/z): 611 ($M + H^+$).

Anal. Calcd. for $C_{20}H_{24}I_2N_2O_2S$: C 39.36; H 3.96; N 4.59. Found: C 39.42; H 4.10; N 4.66.

*4.2.28. 4-{[Benzyl-(5-iodomethyl-4,5-dihydro-thiazol-2-yl)-amino]-methyl}-2,6-di-tert-butyl-phenol hydroiodide (**6p**)*

Yield: 78%; mp: 168-170 °C;

^{1}H NMR (200 MHz, DMSO-d_6): δ = 1.41 (s, 18H, 2×C$(CH_3)_3$), 3.92 (d, J = 6.6 Hz, 2H, NC$\underline{H}_2$CHS), 4.22 (m, 2H, ICH_2), 4.63 (m, 5H, CH_2NCH_2, CHS), 6.86 (c, 1H, OH), 6.96 (c,

2H, H_{arom}), 6.92 (c, 1H, H_{arom}), 7.25 (m, 2H, H_{arom}), 7.34 (m, 3H, H_{arom}), 10.82 (br. s, 1H, NH);

EI-MS (m/z): 679 ($M + H^+$).

Anal. Calcd. for $C_{26}H_{36}I_2N_2OS$: C 46.03; H 5.35; N 4.13. Found: C 46.08; H 5.31; N 4.17.

*4.2.29. Benzyl-furan-2-ylmethyl-(5-iodomethyl-4,5-dihydro-thiazol-2-yl)-amine hydroiodide(**6q**)*

Yield: 80%; mp: 132-135 °C;

^1H NMR (200 MHz, $CDCl_3$): 3.67 (d, J = 6.8 Hz, 2H, NCH_2CHS), 3.98 (dd, J = 3.2, 12.2 Hz, 1H, $ICHH$), 4.17 (dd, J = 7.1, 12.2 Hz, 1H, $ICHH$), 4.52 (m, 1H, CHS), 4.67 (c, 2H, CH_2NCH_2), 4.73 (c, 2H, CH_2NCH_2), 6.37 (dd, J = 2.0, 3.2 Hz, 1H, H_{arom}), 6.47 (d, J = 3.2 Hz, 1H, H_{arom}), 7.23 (d, J = 2.0 Hz, 1H, H_{arom}), 7.30 (m, 5H, H_{arom});

EI-MS (m/z): 541 ($M + H^+$).

Anal. Calcd. for $C_{16}H_{18}I_2N_2OS$: C 35.57; H 3.36; N 5.19. Found: C 35.52; H 3.40; N 5.12.

*4.2.30. (2,3-Dihydro-benzo[1,4]dioxin-6-yl)-(5-iodomethyl-4,5-dihydro-thiazol-2-yl)-amine hydroiodide (**6r**)*

Yield: 78%; mp: 171-173 °C;

^1H NMR (200 MHz, DMSO-d_6): 3.50 (m, 2H, NCH_2), 3.86 (dd, J = 2.9, 11.7 Hz, 1H, $ICHH$), 4.00 (dd, J = 7.3, 11.7 Hz, 1H, $ICHH$), 4.20 (c, 4H, CH_2CH_2), 4.34 (m, 1H, CHS), 6.65 (dd, J = 2.4, 8.6 Hz, 1H, H_{arom}), 6.74 (d, J = 2.4 Hz, 1H, H_{arom}), 6.82 (d, J = 8.6 Hz, 1H, H_{arom});

EI-MS (m/z): 505 ($M + H^+$).

Anal. Calcd. for $C_{12}H_{14}I_2N_2O_2S$: C 28.59; H 2.80; N 5.56. Found: C 28.65; H 2.85; N 5.55.

*4.2.31. (5-Iodomethyl-4,5-dihydro-thiazol-2-yl)-(6-methyl-pyridin-2-yl)-amine hydroiodide (**6s**)*

Yield: 78%; mp: 215-217 °C;

^1H NMR (200 MHz, DMSO-d_6): 2.58 (c, 3H, CH_3), 3.67 (m, 2H, NCH_2CHS), 4.13 (m, 2H, ICH_2), 4.38 (m, 1H, CHS), 7.09 (t, J = 8.5 Hz, 2H, H_{arom}), 7.80 (t, J = 7.8 Hz, 2H, H_{arom});

EI-MS (m/z): 462 ($M + H^+$).

Anal. Calcd. for $C_{10}H_{13}I_2N_3S$: C 26.05; H 2.84; N 9.11. Found: C 26.15; H 2.77; N 9.05.

*4.2.32. Dibenzofuran-3-yl-(5-iodomethyl-4,5-dihydro-thiazol-2-yl)-amine hydroiodide (**6t**)*

Yield: 80%; mp: 200-202 °C;

^{1}H NMR (200 MHz, DMSO-d_6): δ = 3.55 (dd, J = 2.2, 6.8 Hz, 2H, NC$\underline{H}_2$CHS), 3.92 (dd, J = 3.4, 12.0 Hz, 1H, IC$\underline{H}$H), 4.09 (dd, J = 7.3, 12.0 Hz, 1H, ICH$\underline{H}$), 4.38 (m, 1H, CHS), 7.23 (dd, J = 2.0, 8.6 Hz, 1H, H_{arom}), 7.33 (dt, J = 1.2, 7.8 Hz, 1H, H_{arom}), 7.45 (dt, J = 1.2, 7.3 Hz, 1H, H_{arom}), 7.52 (m, 2H, H_{arom}), 7.94 (d, J = 7.8 Hz, 1H, H_{arom}), 8.03 (d, J = 8.3 Hz, 1H, H_{arom});

EI-MS (m/z): 537 ($M + H^+$).

Anal. Calcd. for $C_{16}H_{14}I_2N_2OS$: C 35.84; H 2.63; N 5.22. Found: C 35.89; H 2.71; N 5.19.

4.3. Biological assay

4.3.1. Enzymatic assays

4.3.1.1. In vitro AChE, BChE and CaE inhibition

Acetylcholinesterase (AChE, EC 3.1.1.7, from human erythrocyte, C0663 Sigma), butyrylcholinesterase (BChE, EC 3.1.1.8, from equine serum, C4290 Sigma), carboxylesterase (CaE, EC 3.1.1.1, from porcine liver, E2884 Sigma), acetylthiocholine iodide (ATCh), butyrylthiocholine iodide (BTCh), 5,5´-dithiobis-(2-nitrobenzoic acid) (DTNB), 4-nitrophenol acetate (4-NPA),were purchased from Sigma-Aldrich (Germany).

AChE and BChE activities were measured by the method of Ellman et al. [42]. The assay solution consisted of 0.1 M potassium phosphate buffer pH 7.5, 25°C with the addition of 0.33 mM DTNB, 0.02 unit/mL of AChE or BChE and 1 mM of substrate (acetylthiocholine iodide or butyrylthiocholine iodide, respectively). Assays were carried out with a blank containing all components except ATCh and BTCh in order to account for non-enzymatic reaction.

The activity of CaE was determined spectrophotometrically by the release of 4-nitrophenol at 405 nm [43]. The assay solution consisted of 0.1 M potassium phosphate buffer pH 8.0, 25°C with the addition of 1 mM 4-nitrophenyl acetate and 0.02 unit/mL of CaE. Assays were carried out with a blank containing all components except CaE.

The tested compounds were dissolved in DMSO; the incubation mixture contained 2% (v/v) of the solvent. Eight different concentrations of the test compounds in the range 10^{-12}-10^{-4} M were selected in order to obtain inhibition of AChE and BChE activity between 20% and 80%. The test compounds were added to the assay solution and preincubated at 25^{o}C with the enzymes for 10 min followed by the addition of substrate. A parallel control was made for the assay solution with no inhibitor. Measurements were performed in a BioRad

Benchmark Plus microplate spectrophotometer (France). Each experiment was performed in triplicate. The results were expressed as the mean ± SEM. The reaction rates in the presence and absence of inhibitor were compared, and the percent of residual enzyme activity due to the presence of test compounds was calculated. IC_{50} (the concentration of inhibitor required to decrease the enzyme activity by 50%) values were determined graphically from inhibition curves (log inhibitor concentration vs percent residual enzyme activity) using Origin 6.1 software.

4.3.1.2. Kinetic study of BChE and CaE inhibition. Determination of steady-state inhibition constants.

To elucidate the inhibition mechanisms for the 9 most active compounds, BChE and CaE residual activities were determined in the presence of 3 increasing concentrations of the test compounds and 5-8 decreasing concentrations of the substrates. The test compounds were preincubated with the enzymes at 25°C for 10 min, followed by the addition of the substrates. A parallel control was made for an assay of the rate of hydrolysis of the same concentrations of substrates in the solutions with no inhibitor. The kinetic parameters of substrate hydrolysis were determined. Measurements were performed in a BioRad Benchmark Plus microplate spectrophotometer (France). Each experiment was performed in triplicate. Results were fitted to Lineweaver-Burk double-reciprocal kinetic plots of 1/V versus 1/[S] and values of inhibition constants K_i (competitive component) and αK_i (noncompetitive component) were calculated using the program Origin 6.1.

4.3.2. Cytotoxicity studies

Human fetal mesenchymal stem cells (FetMSC), nonimmortalized fibroblast-like cells obtained from bone marrow of 5- to 6-week-old fetuses [44], were maintained in F12/DMEM medium supplemented with 10% FBS, l-glutamine (3 mM), penicillin 50 IU/ml and streptomycin 50 µg/ml. The FetMSC human fetal mesenchymal stem cell line is a certified culture available from the Russian collection of vertebrate cell cultures of the Institute of Cytology, Russian Academy of Sciences.

To investigate the cytotoxicity of synthetic compounds in FetMSC cells, the 3-(4,5-dimethylthiazol-2yl)-2,5-diphenyl-2H-tetrazoliumbromide (MTT) assay was performed. For the MTT cell viability assay [45], cells were plated in 96-well plates (6×10^3 cells/well) and

allowed to adhere for 24 h. Thereafter, the medium was replaced with fresh medium containing test compounds at different concentrations. Control cells were treated with 0.1% (v/v) DMSO. After 72 h exposure, 0.5 mg/ml of (MTT) was added to each well and the cells were incubated for 4 h. Then, culture medium was aspirated, and MTT-formazan was dissolved in 100% DMSO. MTT staining intensity was read at 570 nm. The MTT staining of control cells was taken as 100%.

4.3.3. Molecular modeling studies

The crystal structure of human BChE (PDB ID 1P0I) [46] was used. Resolution of the structure was 2.00 Å, but it lacked some amino acid residues – Asp378, Asp379 and Gln455, and the Gln486 side chain. All the gaps were located on the protein surface far from the gorge entrance; nevertheless, they were reconstructed according to the procedure outlined by Masson et al [47].

The crystal structure of human CaE (PDB ID 2H7C) [48] was used. Resolution was 2.00Å, but the structure lacked the Glu99 side chain. Although this residue is located rather far from the active site, it was reconstructed manually. This crystal structure contains Coenzyme A in the active site and the gorge, which slightly expands it, making it more favorable for docking of bulky inhibitors.

For both protein structures, all crystallographic waters were removed, along with ligands, ions, and sugars. Hydrogen atoms were added with Reduce [49] software, which protonates histidine rings with regard to the surrounding hydrogen-bonding network.

Marvin Sketch with Calculator Plugins was used for characterizing ligand structures (generating all stereoisomers where possible) and prediction of pK_a of inhibitors (Marvin Sketch 6.0.4, 2013, ChemAxon, http://www.chemaxon.com). Additionally, pK_a values of the most interesting (leading) compounds were predicted by means of ACD/I-Lab (https://ilab.acdlabs.com/iLab2/). The values predicted by the two programs differed significantly; in some cases the pK_a value predicted by one program was more than 7.40 (pH of the experimental measurements), and less than 7.40 by the second one for the same compound (see Supplementary data, Fig. S5). Due to this uncertainty of protonation states of the compounds, both protonation forms of the amidine group of amino-thiazolines were used. With all possible stereoisomers (see Supplementary data, Fig. S5) and protonation states, the library of ligand compounds used in this study included 130 structures.

For all compounds prior to molecular docking, geometry was optimized quantum-mechanically using DFT method B3LYP and basis set 6-31G** carried out with the Gamess-US package [50].

Molecular docking with a Lamarckian Genetic Algorithm (LGA) [51] was performed with Autodock 4.2 [52] software. The grid box for docking included the whole active site and up to the mouth of the gorge of both enzymes. The dimensions used were 15Å × 20.25Å × 18Å for BChE and 19Å × 19Å × 19Å for CaE with grid spacing 0.375 Å. The main LGA parameters were 256 runs, 25×10^6 evaluations, 27×10^4 generations, and population size 300. For the best docked positions an additional 256 runs of local search were performed. Docking positions with the lowest free energies of binding were used for analysis.

Structural images were prepared with Accelrys Discovery Studio Visualiser 3.5 (http://www.accelrys.com).

Acknowledgements

This work was partly supported by grant #14-03-01063 of the Russian Foundation for Basic Research, program "Medicinal Chemistry" of the Russian Academy of Sciences, and a "Dynasty" foundation grant to S.V.L. We thank Dr. Dmitry Suplatov for technical help, the Lomonosov Supercomputer center for computational time, and ChemAxon, Accelrys Software Inc., and ACD Labs, Inc. for free licensing of their products for academic users. We are also grateful to the Center of the Collective-Access Equipment of the Institute of Physiologically Active Compounds, Russian Academy of Sciences for use of equipment (agreement no. 14.621.21.0008, ID no. RFMEFI62114X0008).

References

1. Simon, G. M.; Cravatt, B. F. J. Biol. Chem., **2010**, 285, 11051-11055.
2. Long, J. Z.; Cravatt, B. F. Chem. Rev., **2011**, 111, 6022-6063.
3. Bachovchin, D. A.; Cravatt, B. F. Nat. Rev. Drug. Discov., **2012**, 11, 52-68.
4. Grutzendler, J.; Morris, J. C. Drugs, **2001**, 61, 41-52.
5. Bachurin, S. O. Med. Res. Rev., **2003**, 23, 48-88.
6. Stepankova, S.; Komers, K. Curr. Enzyme Inhib., **2008**, 4, 160-171.
7. Greig, N. H.; Utsuki, T.; Yu, Q.-s.; Zhu, X.; Holloway, H. W.; Perry, T.; Lee, B.; Ingram, D. K.; Lahiri, D. K. Curr. Med. Res. Opin., **2001**, 17, 159-165.
8. Mushtaq, G.; Greig, N. H.; Khan, J. A.; Kamal, M. A. CNS Neurol. Disord. Drug. Targets, **2014**, 13, 1432-1439.
9. Giacobini, E. Int. J. Geriatr. Psychiatry, **2003**, 18, S1-S5.
10. Giacobini, E. Pharmacol. Res., **2004**, 50, 433-440.
11. Greig, N. H.; Utsuki, T.; Ingram, D. K.; Wang, Y.; Pepeu, G.; Scali, C.; Yu, Q. S.; Mamczarz, J.; Holloway, H. W.; Giordano, T.; Chen, D.; Furukawa, K.; Sambamurti, K.; Brossi, A.; Lahiri, D. K. Proc. Natl. Acad. Sci. U. S. A., **2005**, 102, 17213-17218.
12. Lane, R. M.; Potkin, S. G.; Enz, A. Int. J. Neuropsychopharmacol., **2006**, 9, 101-124.
13. Cherif, O.; Allouche, F.; Chabchoub, F.; Chioua, M.; Soriano, E.; Yanez, M.; Cacabelos, R.; Romero, A.; Lopez, M. G.; Marco-Contelles, J. Future Med. Chem., **2014**, 6, 1883-1891.
14. Brus, B.; Kosak, U.; Turk, S.; Pislar, A.; Coquelle, N.; Kos, J.; Stojan, J.; Colletier, J. P.; Gobec, S. J. Med. Chem., **2014**, 57, 8167-8179.
15. Zeb, A.; Hameed, A.; Khan, L.; Khan, I.; Dalvandi, K.; Choudhary, M.; Basha, F. Med. Chem., **2014**, 10, 724-729.
16. Darvesh, S.; Walsh, R.; Kumar, R.; Caines, A.; Roberts, S.; Magee, D.; Rockwood, K.; Martin, E. Alzheimer Dis. Assoc. Disord., **2003**, 17, 117-126.
17. Rafii, M. S.; Walsh, S.; Little, J. T.; Behan, K.; Reynolds, B.; Ward, C.; Jin, S.; Thomas, R.; Aisen, P. S.; Alzheimer's Disease Cooperative, S. Neurol., **2011**, 76, 1389-1394.
18. Winblad, B.; Giacobini, E.; Frolich, L.; Friedhoff, L. T.; Bruinsma, G.; Becker, R. E.; Greig, N. H. J. Alzheimers Dis., **2010**, 22, 1201-1208.
19. Macdonald, I. R.; Rockwood, K.; Martin, E.; Darvesh, S. J. Alzheimers Dis., **2014**, 42, 379-384.
20. Satoh, T.; Hosokawa, M. Chem. Biol. Interact., **2006**, 162, 195-211.
21. Imai, T.; Hosokawa, M. J. Pestic. Sci., **2010**, 35, 229-239.
22. Laizure, S. C.; Herring, V.; Hu, Z.; Witbrodt, K.; Parker, R. B. Pharmacother., **2013**, 33, 210-222.
23. Potter, P.; Wadkins, R. Curr. Med. Chem., **2006**, 13, 1045-1054.
24. Hatfield, M. J.; Potter, P. M. Expert Opin. Ther. Pat., **2011**, 21, 1159-1171.
25. Gaumont, A.-C.; Gulea, M.; Levillain, J. Chem. Rev., **2009**, 109, 1371-1401.
26. Han, F. S.; Osajima, H.; Cheung, M.; Tokuyama, H.; Fukuyama, T. Chemistry, **2007**, 13, 3026-3038.
28. Gawron, O.; Keil, J. Arch. Biochem. Biophys., **1960**, 89, 293-295.
29. Andreani, A.; Burnelli, S.; Granaiola, M.; Guardigli, M.; Leoni, A.; Locatelli, A.; Morigi, R.; Rambaldi, M.; Rizzoli, M.; Varoli, L.; Roda, A. Eur. J. Med. Chem., **2008**, 43, 657-661.
30. Boltneva, N. P.; Serebryakova, O. G.; Makhaeva, G. F.; Serkov, I. V.; Proshin, A. N.; Bachurin, S. O. Dokl. Biochem. Biophys., **2013**, 451, 209-211.

31. Trofimova, T. P.; Pushin, A. N.; Proshin, A. N.; Stash, A. I.; Mandrugin, A. A.; Fedoseev, V. M.; Proskuryakov, S. Y. Chem. Heterocycl. Comp., **2007**, 43, 370-376.
32. Tkachenko, S. E.; Pushin, A. N.; Fedoseev, V. M. Zh. Obshch. Khim., **1987**, 57, 2400-2401.
33. Zontova, V. N.; Koroleva, T. I.; Mel'nikov, N. N.; Grapov, A. F. Zh. Obshch. Khim., **1990**, 60, 798-804.
34. Fedoseev, V. M.; Churilin, V. S.; Tashchi, V. P. Dokl. Acad. Nauk USSR, **1971**, 197, 1351-1352
35. Tsurkan, L. G.; Hatfield, M. J.; Edwards, C. C.; Hyatt, J. L.; Potter, P. M. Chem. Biol. Interact., **2013**, 203, 226-230.
36. Makhaeva, G. F.; Serebryakova, O. G.; Boltneva, N. P.; Galenko, T. G.; Aksinenko, A. Y.; Sokolov, V. B.; Martynov, I. V. Dokl. Biochem. Biophys., **2008**, 423, 352-357.
37. Makhaeva, G. F.; Radchenko, E. V.; Baskin, I. I.; Palyulin, V. A.; Richardson, R. J.; Zefirov, N. S. SAR QSAR Environ. Res., **2012**, 10.1080/1062936x.2012.679690 1-21.
38. Makhaeva, G. F.; Radchenko, E. V.; Palyulin, V. A.; Rudakova, E. V.; Aksinenko, A. Y.; Sokolov, V. B.; Zefirov, N. S.; Richardson, R. J. Chem. Biol. Interact., **2013**, 10.1016/j.cbi.2012.10.012.
39. Rudakova, E. V.; Boltneva, N. P.; Makhaeva, G. F. Bull. Exp. Biol. Med., **2011**, 152, 73-75.
40. Mooibroek, T. J.; Gamez, P. CrystEngComm, **2013**, 15, 4565.
41. Riley, K. E.; Hobza, P. Phys. Chem. Chem. Phys., **2013**, 15, 17742-17751.
42. Ellman, G. L.; Courtney, K. D.; Andres, V., Jr.; Feather-Stone, R. M. Biochem. Pharmacol., **1961**, 7, 88-95.
43. Sterri, S. H.; Johnsen, B. A.; Fonnum, F. Biochem. Pharmacol., **1985**, 34, 2779-2785.
44. Krylova, T. A.; Koltsova, A. M.; Zenin, V. V.; Musorina, A. S.; Yakovleva, T. K.; Poljanskaya, G. G. Cell Tissue. Biol., **2012**, 6, 95-107.
45. Mosmann, T. J. Immunol. Methods, **1983**, 65, 55-63.
46. Nicolet, Y.; Lockridge, O.; Masson, P.; Fontecilla-Camps, J. C.; Nachon, F. J. Biol. Chem., **2003**, 278, 41141-41147.
47. Masson, P.; Lushchekina, S.; Schopfer, L. M.; Lockridge, O. Biochem. J., **2013**, 454, 387-399.
48. Bencharit, S.; Edwards, C. C.; Morton, C. L.; Howard-Williams, E. L.; Kuhn, P.; Potter, P. M.; Redinbo, M. R. J. Mol. Biol., **2006**, 363, 201-214.
49. Word, J. M.; Lovell, S. C.; Richardson, J. S.; Richardson, D. C. J. Mol. Biol., **1999**, 285 1735-1747.
50. Schmidt, M. W.; Baldridge, K. K.; Boatz, J. A.; Elbert, S. T.; Gordon, M. S.; Jensen, J. H.; Koseki, S.; Matsunaga, N.; Nguyen, K. A.; Su, S.; Windus, T. L.; Dupuis, M.; Montgomery, J. A. J. Comput. Chem., **1993**, 14, 1347-1363.
51. Morris, G. M.; Goodsell, D. S.; Halliday, R. S.; Huey, R.; Hart, W. E.; Belew, R. K.; Olson, A. J. J. Am. Chem. Soc., **1998**, 19, 1639-1662.
52. Morris, G. M.; Huey, R.; Lindstrom, W.; Sanner, M. F.; Belew, R. K.; Goodsell, D. S.; Olson, A. J. J. Comput. Chem., **2009**, 30, 2785-2791.

Figure Captions:

Figure 1. General structure of compounds in the present study. X = Br or I; R^1 = substituted or unsubstituted aryl or aralkyl; R^2 = H, aryl, or aralkyl. Syntheses are depicted in **Scheme 1** and structures of individual compounds are listed in **Table 1**.

Figure 2. Design strategy for the new series of *N,N*-disubstituted 2-aminothiazolines of general formula shown in Fig. 1. X = Br or I. Syntheses are depicted in **Scheme 1** and structures of the compounds are presented in **Table 1**. Proposed interactions of compounds with active site residues of target enzymes include the following, illustrated with selected compounds: (**a**) Halogen and aromatic (benzyl, pyridine) fragments are intended to have stacking interactions with aromatic Trp, Phe and Tyr residues, primarily the most favorably oriented Trp82 and Trp231 of BChE; (**b**) Alkyl fragments are intended to interact with numerous hydrophobic residues lining the gorge of CaE; (**c**) Positively charged groups are intended to interact with Glu of both enzymes (Glu197 of BChE and Glu220 of CaE), and probably Asp70 of the peripheral anionic site of BChE; (**d**) Electronegative atoms (N, O) are expected to interact with the oxyanion hole of both enzymes (Gly116/Gly117/Ala199 for BChE and Gly142/Gly143/Ala222 for CaE).

Figure 3. Steady state inhibition of BChE by compounds **5h** (**A**) and **6h** (**B**). Lineweaver-Burk reciprocal plots of initial velocity and substrate concentrations in the presence of inhibitors **5h, 6h** (three concentrations) and their absence are presented. Plot **A** shows competitive inhibition and plot **B** shows mixed-type inhibition.

Figure 4. Steady state inhibition of CaE by compounds **5h** (**A**) and **6h** (**B**). Lineweaver-Burk reciprocal plots of initial velocity and substrate concentrations in the presence of inhibitors **5h, 6h** (three concentrations) and their absence are presented. Plots **A** and **B** show non-competitive inhibition.

Figure 5. Binding positions of compounds **5h** (carbon atoms are colored grey) and **6h** (carbon atoms are colored blue) inside the gorge of human CaE (**A**) and BChE (**B**). Carbon atoms of the enzyme residues side chains are colored green and the catalytic residues are depicted in cyan.

Figure 6. Binding positions of compounds **5l** (carbon atoms are colored grey) and **6l** (carbon atoms are colored blue) in the active site of BChE. (**A**) and (**B**) are views from different vantage points. In panel (**A**) carbon atoms of BChE residues side chains are colored green and the catalytic residues are rendered in cyan; in panel (**B**) BChE solvent accessible surface and van der Waals spheres of the inhibitor halogen atoms are shown.

Figure 7. Binding positions of compounds **5i** (carbon atoms are colored grey) and **6i** (carbon atoms are colored blue) inside the gorge of human CaE (**A**) and BChE (**B**). Carbon atoms of the enzyme residues side chains are colored green and the catalytic residues are depicted in cyan.

Figure 8. Summary of compounds found to be selective inhibitors of BChE, both BChE and ChE, or CaE.

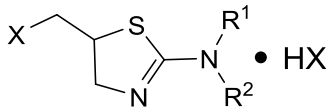

Fig. 1

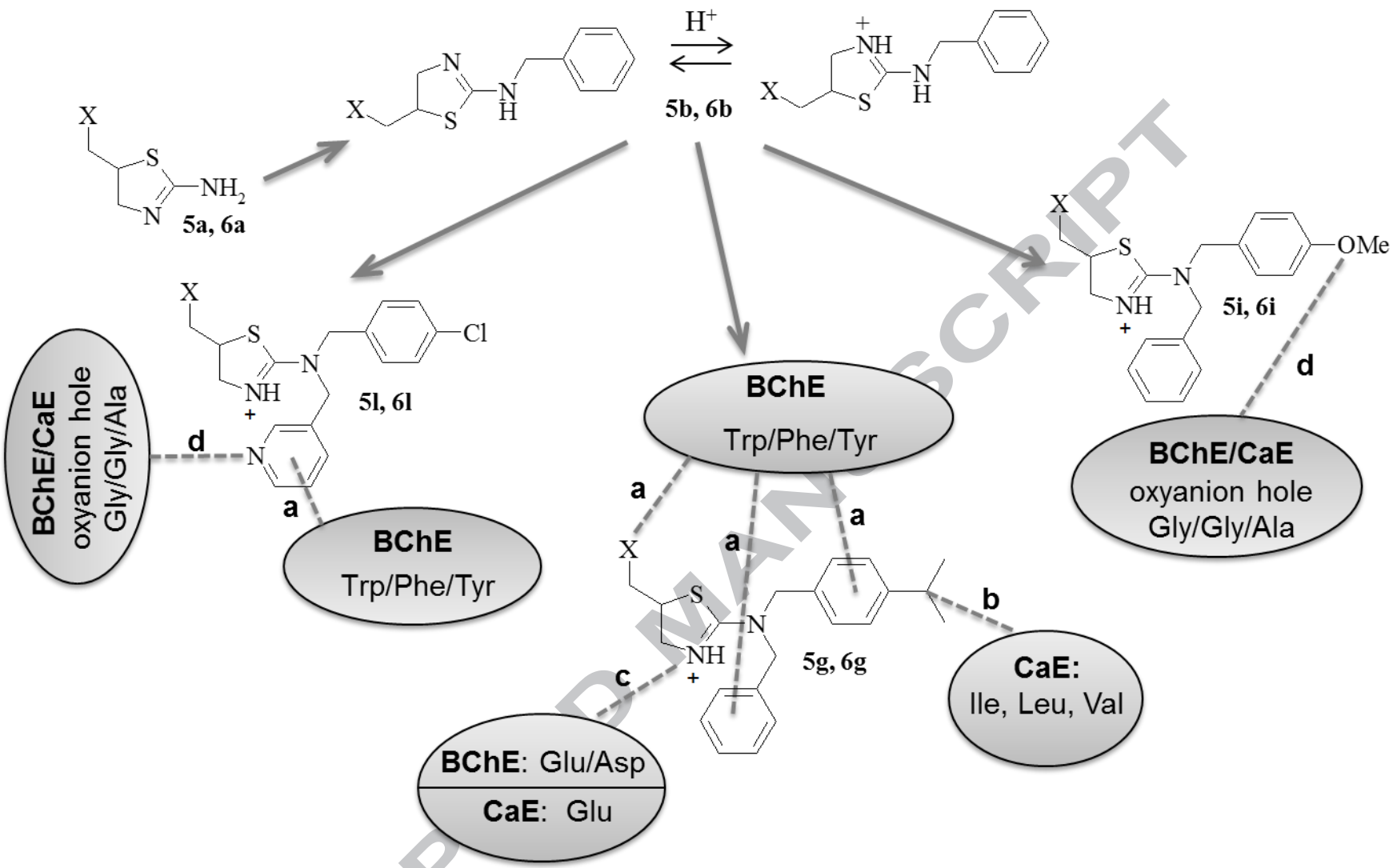

Fig. 2

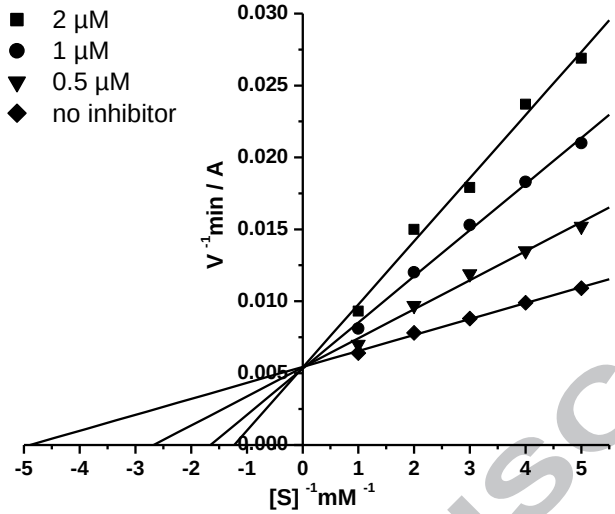

A

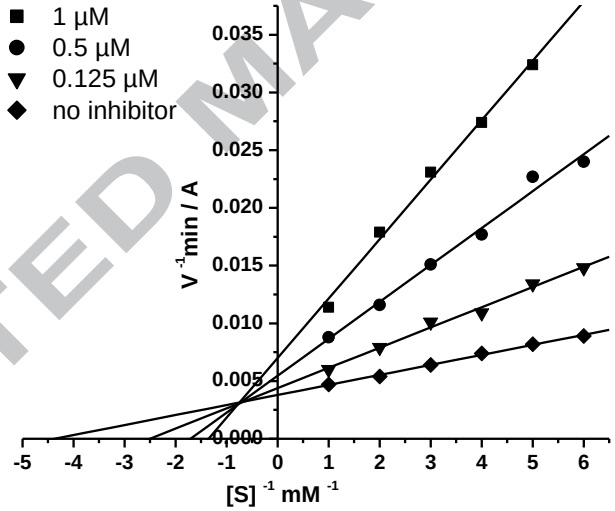

B

Figure 3.

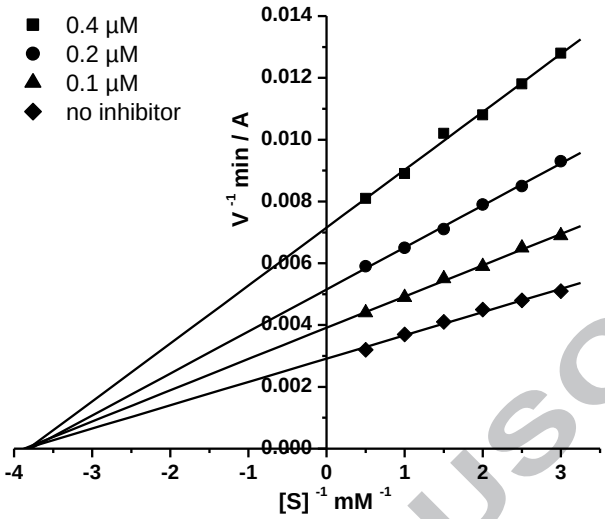

A

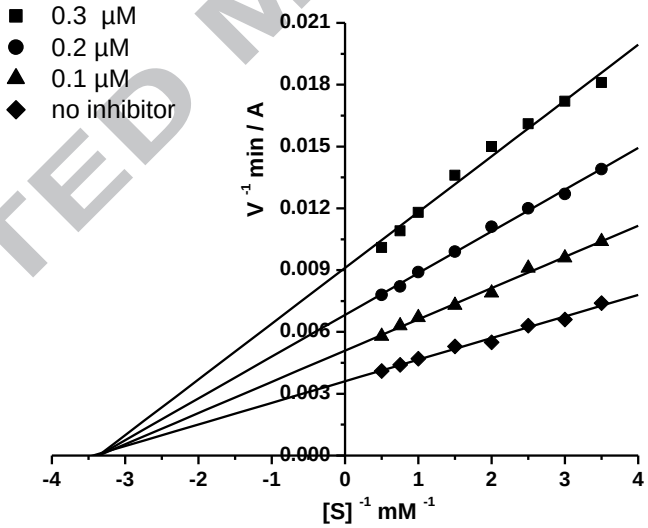

B

Figure 4.

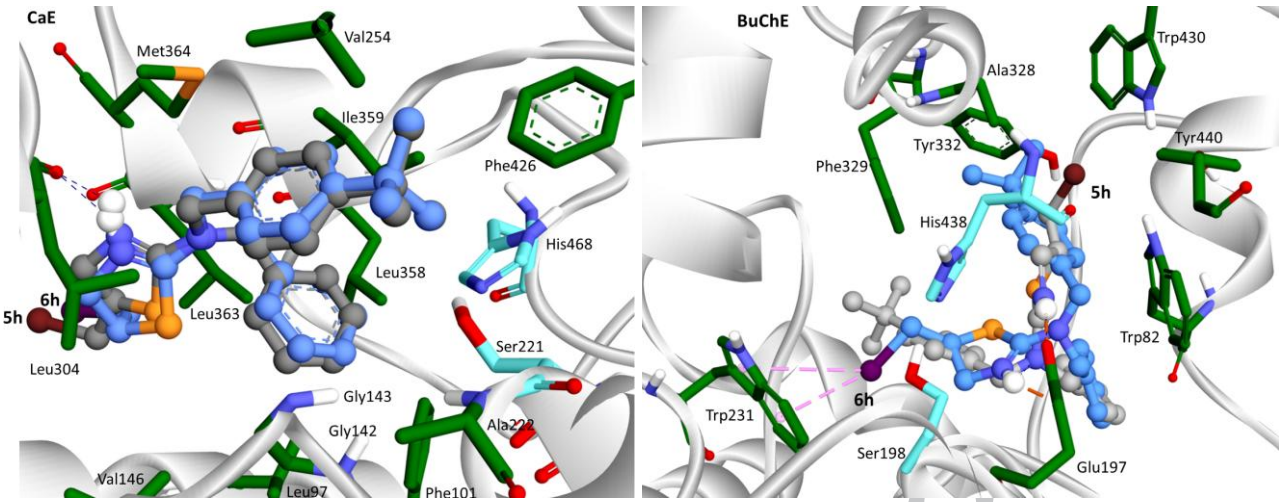

A **B**

Figure 5.

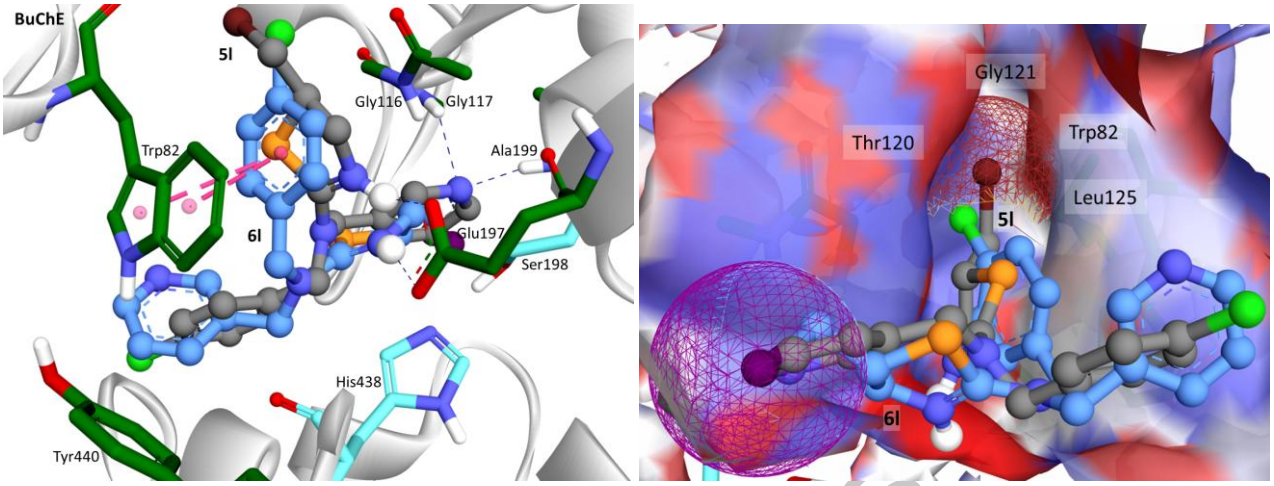

A **B**

Figure 6.

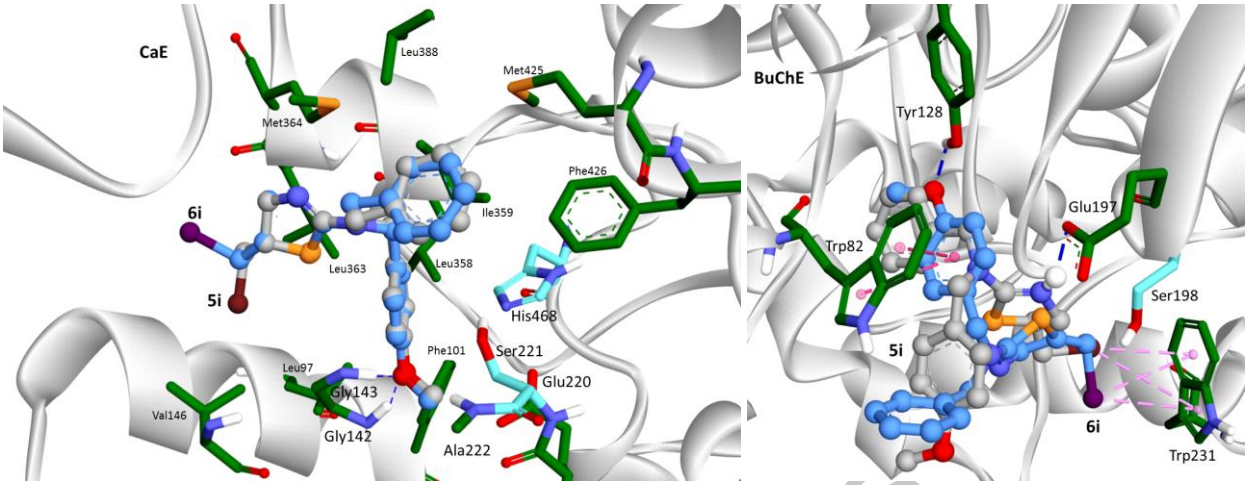

A **B**

Figure 7.

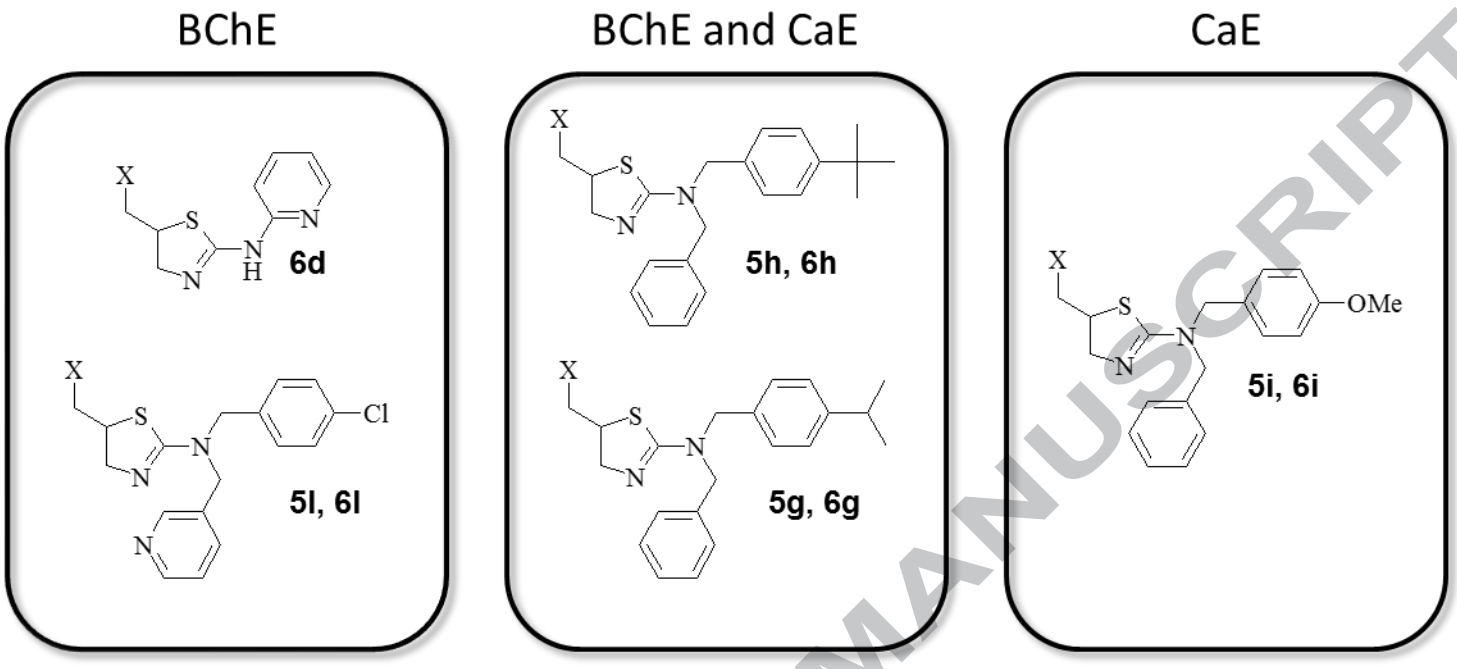

Fig. 8

Graphical abstract